

NIST GCR 11-951

**Ignition Propensity of Hydrogen in the
Presence of Metal Surfaces**

NIST GCR 11-951

Ignition Propensity of Hydrogen in the Presence of Metal Surfaces

Chih-Jen Sung¹
James S. T'ien²
Kyle Brady¹

¹Department of Mechanical Engineering
University of Connecticut
Storrs, CT 06269

²Department of Mechanical and Aerospace Engineering
Case Western Reserve University
Cleveland, OH 44106

Grant 60NANB7D6150

November 2011



U.S. Department of Commerce
John E. Bryson, Secretary

National Institute of Standards and Technology
Patrick D. Gallagher, Under Secretary of Commerce for Standards and Technology and Director

Notice

This report was prepared for the Engineering Laboratory of the National Institute of Standards and Technology under Grant number 60NANB7D6150. The statement and conclusions contained in this report are those of the authors and do not necessarily reflect the views of the National Institute of Standards and Technology or the Engineering Laboratory.

**Final Report of a Research Program on
Department of Commerce Grant 60NANB7D6150**

Entitled

Ignition Propensity of Hydrogen in the Presence of Metal Surfaces

Prepared by

Professor Chih-Jen Sung¹
Professor James S. T'ien²
Mr. Kyle Brady¹

¹Department of Mechanical Engineering
University of Connecticut
Storrs, CT 06269

²Department of Mechanical and Aerospace Engineering
Case Western Reserve University
Cleveland, OH 44106

October 13, 2011

1. Introduction

Hydrogen as an energy carrier has received much attention in recent years as a result of a confluence of economic, environmental, and political pressures on the continued use of fossil fuels. The benefits of using hydrogen fuel over fossil fuel products are numerous and well known, most prominently (but not limited to) improved air quality. Many studies on this subject have been published addressing the public health concerns surrounding fossil fuel use, concluding almost universally that particulates and other components of fossil fuels in the air contribute to morbidity and mortality in humans. In addition to human health problems, there is the growing concern that continued widespread use of carbon-based fuels may contribute to world-wide climate change.

Hydrogen, depending upon its source, can reduce or eliminate many of these problems as its combustion in an engine or use in a fuel cell emits no carbon emissions in gaseous or particulate form, and can be produced free of sulfur to avoid SO_x emissions causing acid rain. Despite these apparent benefits, hydrogen fuel is still perceived as a safety hazard, and past disasters attributed to hydrogen flammability have only strengthened the common perception of hydrogen as a dangerous fuel. It has therefore been the goal of this study to help determine potential safety hazards associated with hydrogen fuel, specifically considering a catalytic ignition source. As such, the objectives of this investigation are as follows.

- (1) Investigate the activity of a known catalyst for a wide range of hydrogen/air mixtures.
- (2) Investigate the possibility of catalytic activity from common metals and their oxides.
- (3) Investigate the impact of catalyst configurations on observed activity.
- (4) Investigate how an active catalyst behaves under simulated leakage scenarios.

1.1 Experiments Conducted under This Study

The following represents a brief description of the activities conducted under this experimental study as well as the motivation for each experiment.

1.1.1 Stagnation-Point Flow Experiment

The stagnation-point flow experiment represents a well-characterized combustion system that has been used extensively to determine combustion properties of fuels as well as the activity of catalysts. In this way, the ignition characteristics of a hydrogen/air-catalyst system can be determined for a range of flow parameters and mixtures, and for a range of metallic stagnation plates. Using this information, potentially active metallic samples for initiating ignition can be identified, and dangerous conditions (from a fire safety perspective) can be avoided.

1.1.2 Catalytic Microtube Experiment

The intent of this experiment is to elucidate the impact of varied configurations on the ignition and activity of catalytic samples. Based upon the results of the stagnation-point flow experiments, a limited number of metals are tested in this configuration.

1.1.3 Scaled Garage Experiment

For both stagnation-point and microtube experiments, the goal is to determine ignition temperatures for hydrogen/air systems under a variety of flow conditions. In these cases, mixtures are explicitly flowed past a catalytic surface. Of equal or greater importance to fire safety, however, is the activity when hydrogen is simply leaked into an enclosed

space where a catalytic substance may be present. This type of situation is modeled within the simulated garage experiment, using a 1/16th linear scale model of a “typical” two-car garage. This system facilitates the investigation of the effects of flow rate, catalyst position, and venting on any surface reactions, and aids in investigating the possibility of surface reactions transitioning into the gas phase, causing an explosion.

1.2 Organization of This Report

Section 2 describes the apparatus and methods used for each of the three experiments listed above. The results of each of these experiments are separately discussed in Section 3, and concluding remarks based upon the experimental results as an aggregate are presented in Section 4.

2. Methods and Apparatus

2.1 Stagnation-Point Flow Apparatus

The apparatus used for this portion of the study consists of a burner assembly generating laminar flows, a catalytic stagnation plate and its heating control unit, a flow control system, and a Rainbow Schlieren Deflectometry (RSD) visualization system. A flow diagram describing the details of this apparatus has been provided in Fig. 1. Supplemental reference figures describing the stagnation-point flow apparatus can be found in Appendix A.

2.1.1 Flow Control and Mixing

The flow to the stagnation surface is provided by a contoured nozzle used in previous studies for the determination of laminar flame speeds of various fuels. It has been modified for this study with the addition of stainless-steel fine mesh inserts that serve the dual function of aiding in the prevention of flashback to the flow control system as well as preventing jetting of the flow within the nozzle itself. The exit of the nozzle has a diameter of 10.4 mm, which is internal to an inert shroud co-flow that helps stabilize a flame away from the nozzle exit in the event of a gas-phase flame.

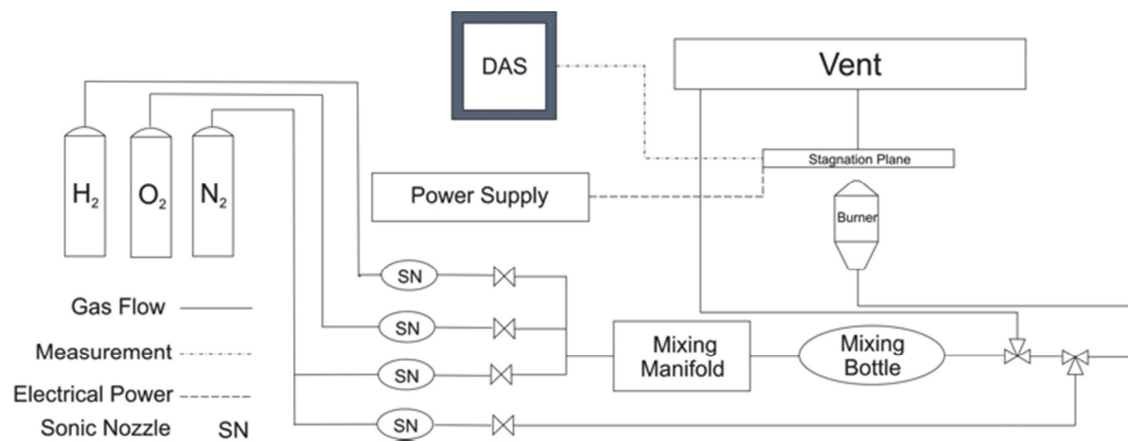


Figure 1: Flow diagram of the stagnation-point flow experiment.

In an effort to minimize transient concentrations impinging on the surface during experiment startup, two separate flows are provided to the burner via a system of two manually-operated three-way valves as shown in Fig. 1. The first flow consists of the pre-mixed $H_2/O_2/N_2$ gases, while the second consists of a pure nitrogen flow. In the “Off” position, the valves redirect the premixed flow directly to the exhaust hood, while nitrogen gas flows through the burner assembly and impinges on the catalyst surface. In the “On” position, the nitrogen gas is shut off, while the pre-mixed gas flows through the

burner. This system provides for a need to isolate the platinum surface from room air so as to minimize the possibility of initial adsorbed oxygen or contaminants on the catalyst surface. In addition, by allowing the premixed gases to flow continuously prior to catalytic experiments, transient equivalence ratio effects are minimized.

2.1.2 Stagnation Assembly

The stagnation surface is shown diagrammatically in Fig. 2, and consists of a support, a heating assembly, temperature measurement, and a platinum or other metallic foil. The ceramic used for the ceramic support is an unfired alumina silicate ceramic purchased from McMaster-Carr, of dimensions 4 in \times 4 in \times 3/8 in. This ceramic is chosen for its easy machinability and resistance to cracking. To accommodate the foil, heater, and thermocouples, a 1 in square hole is machined through the center of the ceramic plate.

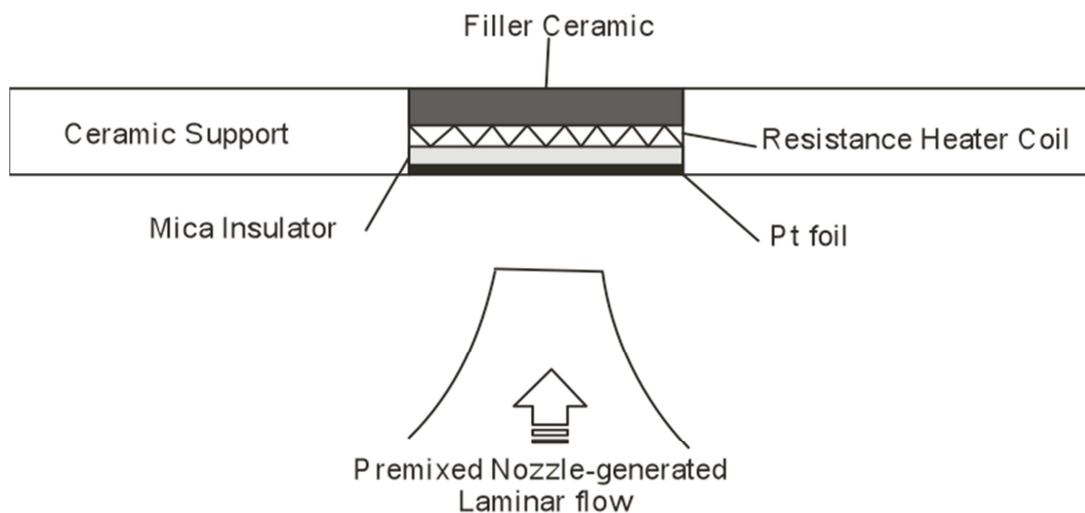


Figure 2: Schematic view of the stagnation assembly.

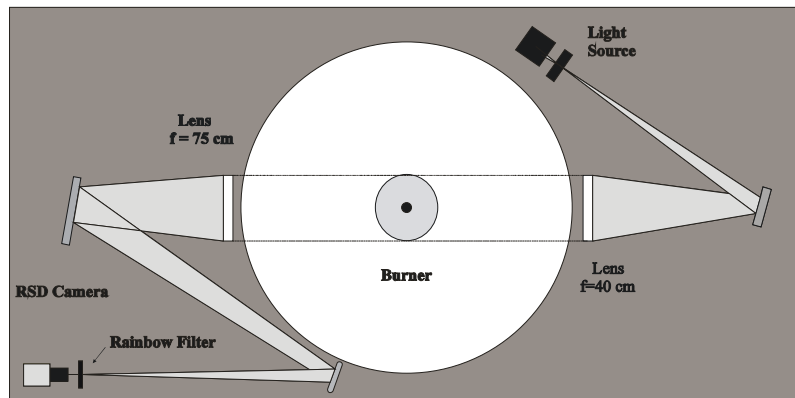
The heating assembly is constructed in-house using nickel-chromium heating wire purchased from Omega Engineering with a resistance of 6.617 Ω /ft and a high-alumina

ceramic sheet purchased from McMaster-Carr of dimensions 1 in \times 1 in \times 0.04 in. The heating wire is wrapped uniformly around the ceramic sheet to form a heating element and is sandwiched between phlogopite mica sheets in order to electrically isolate the heater from the thermocouples. In a similar fashion, the platinum foil and thermocouples are combined into a single assembly by sandwiching five thermocouples in a typical dice pattern (one in each of four corners and one in the center) between the platinum foil and mica sheeting using high-temperature ceramic cement. These elements are then combined into the ceramic plate as a completed assembly, as shown in Fig. 2.

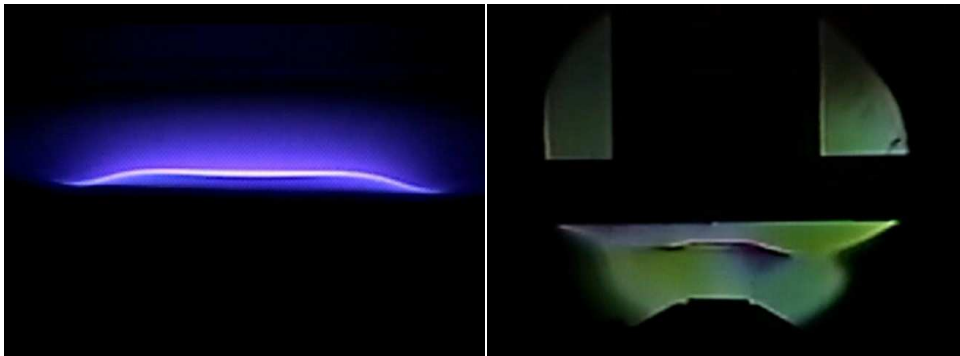
2.1.3 Rainbow Schlieren Deflectometry Visualization System

A visualization system is implemented in this study out of a necessity for determining when a gas-phase flame develops both for safety and data acquisition purposes. For the premixed H₂/air system under lean conditions, this is complicated by the fact that the hydrogen flame will not emit visible light. Methane addition was initially considered to render the gas-phase flame visible, but it was discovered that, even in trace amounts, methane inhibited the catalytic activity of the H₂/air system. As a result, a Rainbow Schlieren Deflectometry (RSD) technique is adopted and is illustrated in Fig. 3(a). The light source is a 150 W halogen lamp and its output is guided to a proper location using a 600 μ m diameter fiber optic cable. A 50 μ m wide vertical slit is positioned at the end of the fiber and serves as a point source. Because of the limited space available, the focal length of the focusing lens is restricted to 75 cm. Figure 3(b) shows and compares sample methane/air and hydrogen/air flames as seen using both direct imaging (left) and RSD imaging (right). The figure demonstrates the ability to image the flame using RSD even for the “invisible” hydrogen case.

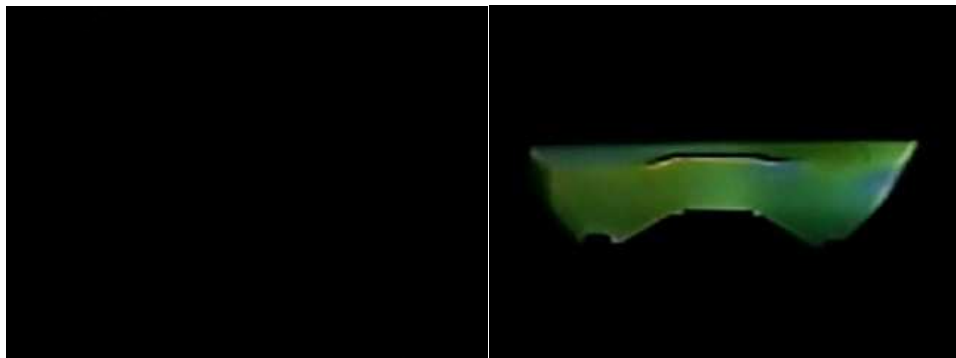
a)



b)



Methane Flame



Hydrogen Flame

Figure 3: (a) Schematic view of the Rainbow Schlieren Deflectometry system. (b) Typical visual (left) and RSD (right) images observed for methane/air and hydrogen/air flames. Comparison reveals that observation of a hydrogen flame is only made possible with this optical technique.

2.2 Catalytic Microtube Apparatus

This experiment is designed to model the effects of residence time and equivalence ratio on the catalytic ignition characteristics of the H₂/air system. The system consists of a flow control system, tubular reactor test section located in an isolation chamber, and a data acquisition system. A realistic application of this geometric situation may be a flow through a confined space containing catalytic material, such as a catalytic converter. Two sets of data are taken in this configuration; a very low flow rate set using a 0.8 mm Pt tube, and a higher flow rate set intended to have comparable residence times to the lowest stretch-rate end of the stagnation-point flow data.

2.2.1 Flow Control and Mixing

The flow control system for the tubular reactor experiment is functionally identical to the stagnation-point flow experiment, and is shown schematically in Figure 4.

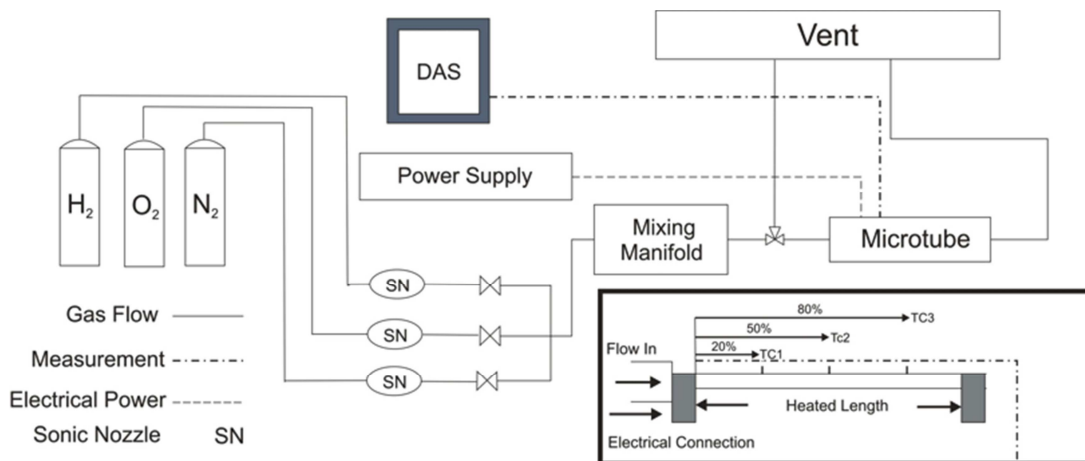


Figure 4: Flow diagram of the tubular reactor system.

Mixing is accomplished via a mixing manifold, which introduces oxygen and hydrogen flows perpendicularly to a nitrogen flow. Since the flow rates used in this

experiment are very low as a result of the diameter of the catalytic microtube, no additional mixing is provided, as the increased dead volume would result in significant lag time between flow composition changes and the flow reaching the reactor.

2.2.2 Tubular Reactor

The tubular reactor for this experiment is in two configurations; a 0.4 mm and 0.8 mm inner diameter (ID) metallic tube with a nickel tab attached near each end. The 0.4 mm ID tube has a wall thickness of 0.15 mm and a length of 100 mm, 70 mm of which is heated. The 0.8 mm ID tube has a wall thickness of 0.1 mm and a length of 200 mm, 140 mm of which is resistively heated. Although these tube choices are partially dictated by the availability of platinum tubing, the heated length is determined based on maintaining a constant aspect ratio (length by inner diameter) between the two tubes in an effort to aid with comparison between the two configurations. Three thermocouples, TC1, TC2, and TC3, are attached to the outside of each tube. For the 0.4 mm tube, these are attached at 20%, 50%, and 73% of the heated length. For the 0.8 mm tube, the attachment points are at 20%, 50%, and 80% of the heated length. The attachment points approximately break the tube lengths into quarters, though the 0.4 mm tube required repairs that necessitated changing the attachment point of TC3 to 73%. The thermocouples are mounted to the tube via tack welding at the discretion of the instrumentation shop at NASA Glenn Research Center. Examples of the tubes and their mounting method are provided as supplemental figures in Appendix B.

The nickel tabs attached to each tube facilitate mounting of the tube and connection to a DC power supply. To further facilitate mounting, stainless steel tubes are brazed to

the ends of the platinum tube, which allows for Swagelok connection to the flow system. The Sorenson DCR80-33B DC power supply is used to directly heat the metal tube via resistive heating using voltage control. This supply has a 100V/33A maximum output, though only a fraction of full capacity is necessary for this study.

2.2.3 Testing Procedure

With the tube at room temperature, the premixed flow is passed to the tube inlet so that H₂/air is passing through the test section. If the mixture does not immediately exhibit any sort of surface activity, the voltage from the DC power supply is slowly incremented until surface activity or an ignition event is observed. Once this event occurs, the tube is allowed to come to a steady-state (if applicable), at which point the voltage is removed and a new steady-state temperature profile emerges. If removal of voltage from the tube length does not extinguish reactions, surface activity is quenched by switching the H₂/air flow back to vent, effectively stopping flow within the test section.

2.3 Scaled Garage Experiment

This experiment is designed to observe the interaction of hydrogen/air mixtures with a catalytic substance under conditions commensurate with leakage into an enclosed space containing a catalytic ignition source. Specifically, this configuration is designed to test the behavior of the catalyst under conditions that might be similar to leakage from a hydrogen-fueled vehicle into a garage setting. Whereas previous experiments addressed the condition of a combustible flow past a catalytic substance, this experiment attempts to address the situation where flow against the catalytic surface is minimal or negligible.

2.3.1 Flow Control and Mixing

As with the previous experiments, flow control is accomplished by calibrated sonic nozzles. For this case, compressed air and/or hydrogen are used in experimentation, while flow control is otherwise functionally identical to that provided in Figs. 1 and 4.

2.3.2 Scaled Garage Chamber

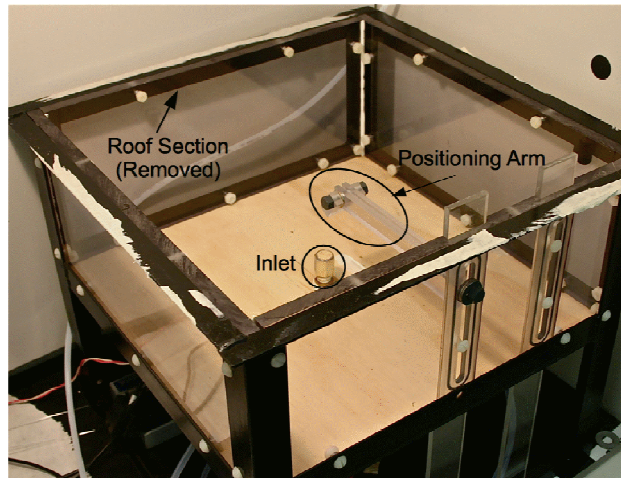
The intent of this study is to investigate the hazards associated with the presence of a catalyst within an enclosure containing accumulated hydrogen. As a result, a model of a two-car garage is chosen as it represents a situation where a hydrogen release may be likely to occur. For the purposes of this study, “typical” dimensions are chosen as 6.096 m × 6.096 m × 3.048 m (20 ft × 20 ft × 10 ft). In order to keep the combustible volume to a manageable level for safety purposes, a 1/16th linear scale factor of this model is chosen, resulting in interior dimensions of 38.1 cm × 38.1 cm × 19.05 cm (15 in × 15 in × 7.5 in). For visibility, the walls of the test chamber are constructed of clear polycarbonate plastic, which can be easily replaced to incorporate varied venting scenarios, while the “roof” is constructed using a plastic covering designed to be able to burst away as a result of a pressure rise inside the chamber. This last feature is in place to allow gases to quickly rupture the roof section in the event of ignition to avoid a dangerous pressure buildup. The inlet for gases is located in the center of the floor, and consists of a compressed air muffler that acts as a diffusing device. Venting for the garage is provided in the form of vents located in one corner at the top and/or bottom of a wall. With the exception of the results presented in Section 3.3.3, the venting configuration is a pair of 0.25 inch diameter holes, the top hole centered 1 inch from the roof, and 0.75 inch from the corner,

and the bottom hole located 0.75 inch from both the floor and corner. The garage system is shown photographically and diagrammatically in Figs. 5(a) and 5(b), respectively.

The catalyst used is a 25 mm × 25 mm × 0.1 mm platinum foil of 99.95% purity (not shown in Fig. 5(a)) purchased from the Goodfellow Corporation and is also used in the stagnation flow configuration. This foil can be mounted within the chamber at various positions by way of a polycarbonate positioning arm attached to a moveable section within the front wall, and surface temperature is monitored continuously via a centrally located K-type thermocouple connected to a National Instruments SCXI-1101 sampling at 10 Hz. Hydrogen measurement is accomplished in this system by way of an array of four TCG-3880 hydrogen sensors purchased from Xensor Integration. These sensors, embedded within the interior wall of the chamber, measure the thermal conductivity of the gas mixture, from which a measurement of the concentration of hydrogen can be made as a result of the large difference in thermal conductivity between hydrogen and air.

The flow system used in this study consists of sonic nozzle flow control for two situations; H₂/air mixtures to aid with comparison of experimental results from the stagnation-point flow configuration, and pure H₂ to simulate a practical leakage scenario. For the first scenario, H₂ and air are combined in the molar ratio of H₂/air = $\Phi/2.38$ for equivalence ratio Φ . Thorough mixing is accomplished ahead of the inlet via a mixing manifold connecting the three separate metered flows as well as a subsequent mixing section. For all results presented here, the platinum foil is oriented horizontally, with the reactive surface facing downward.

a)



b)

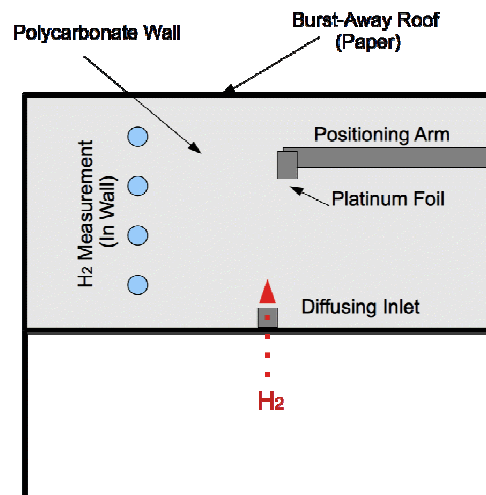


Figure 5: (a) Photograph of simulated garage chamber including positioning arm and diffusing inlet. The burst-away roof is removed for clarity. (b) Diagram of simulated garage apparatus.

2.3.3 Testing Procedure

Testing begins with the platinum foil at approximately room temperature, with only slight elevations (< 10 K) as a result of residual heat allowed. Using adhesive tape, the roof section is sealed and a hydrogen/air mixture at a given equivalence ratio (or hydrogen alone) is allowed to flow into the chamber. The chamber is allowed to remain in this

condition until both surface temperature and hydrogen mole fraction have reached a steady state. At the end of testing, the flow into the chamber is ceased, and the plastic roof material removed. The catalyst surface is allowed to cool to room temperature before commencing a subsequent test.

3. Results and Discussion

3.1 Stagnation-Point Flow Experiment

3.1.1 Platinum Experiments

This series of experiments was conducted in order to determine the behavior of a highly active catalyst in a hydrogen-air system. This combination represents a “worst-case scenario” from a fire safety perspective with respect to catalytic materials.

3.1.1.1 Characteristic Ignition Response for a Platinum Surface

Figure 6 shows the characteristic response for an example case of $\Phi = 0.8$ and stretch rate $k = 300 \text{ s}^{-1}$, with important events marked. A single imposed power of 7.2 W is utilized, with heat input starting at reference time $t = 0$. In addition to a characteristic reactive response, a non-reactive response for a flow containing only nitrogen and hydrogen is provided for comparison. By removing oxygen and replacing with nitrogen, a gas mixture with approximately equal heat transfer properties can be produced, and is used to exemplify and identify the individual effects of surface reactions and external heat addition during the induction period. In contrast to the H_2/N_2 case, which reaches approximately steady state (within 5 K) in the first ~150 seconds, the surface temperature

for the H_2 /air case gradually increases up to the ignition point, at which time the surface reactions rather than the external heat input become the dominant contributor to surface temperature rise. This ignition point is given as the catalytic ignition temperature (T_C) and is defined by the intersection of least-squares regression fit lines fitted to the induction region and the thermal runaway region of the temperature response plot. This definition is chosen as it relates the pre-ignition heat release behavior in the induction region to the thermal runaway behavior. By defining T_C in this way, it avoids the complications of variable transient responses that occur upon reactant introduction at elevated surface temperatures, which may introduce large errors in determining T_C .

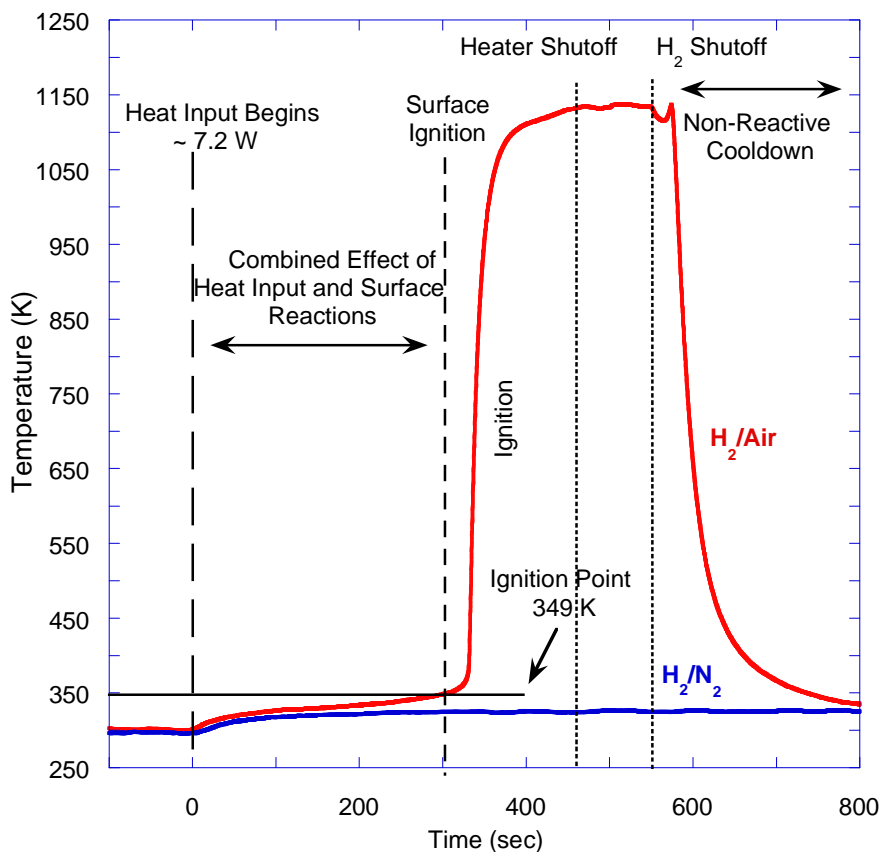


Figure 6: Typical temperature history of a hydrogen/air mixture impinging on a platinum surface compared to a similar mixture comprised of nitrogen and hydrogen only. Conducted for $\Phi = 0.8$, $k = 300 \text{ s}^{-1}$, and an external heat input of $\sim 7.2 \text{ W}$.

Figure 6 further shows that after the point of ignition, thermal runaway is observed in the form of rapid surface temperature increase. Following thermal runaway, the surface temperature is seen to reach approximately steady-state. Subsequently, heater power is removed to examine the dependence of surface reactivity on external heat input. As is noted in Fig. 6, no discernable drop in surface temperature is observed, indicating both that the surface reactions are self-sustaining and that the contribution to the steady-state surface temperature from external heating is negligible. Additional tests where the heat input is eliminated just after T_C is reached (not shown) differ negligibly from the case shown, indicating that the surface reactions are self-sustaining over the entire post-ignition regime, including during the thermal runaway period.

It is also noted that for the cases requiring external heating for catalytic ignition, there exists a critical heat input value beyond which thermal runaway can be observed. Figure 7 shows the surface temperature evolution profiles at five different heat input values for $\Phi = 0.4$ and $k = 400 \text{ s}^{-1}$. These cases are overlaid such that thermal input occurs at time $t = 0$ so that the induction region temperature histories for each case can be compared. As observed in Fig. 5, minimum external energy is necessary in order to ignite the mixture on the surface, for these conditions between 5.6 W and 7.2 W. Exceeding this critical power reduces the induction time between the initial heat input and the ignition time demarcating the beginning of thermal runaway. It is also seen that as the initial heat input becomes progressively larger, the ignition point T_C becomes more difficult to differentiate as the beginning of thermal runaway merges with the effects of electrical heat input. This result implies that the catalytic ignition temperature T_C is best determined by the minimum input power necessary that results in thermal runaway. As such, the

corresponding minimum heat input case is used to determine all subsequent ignition data.

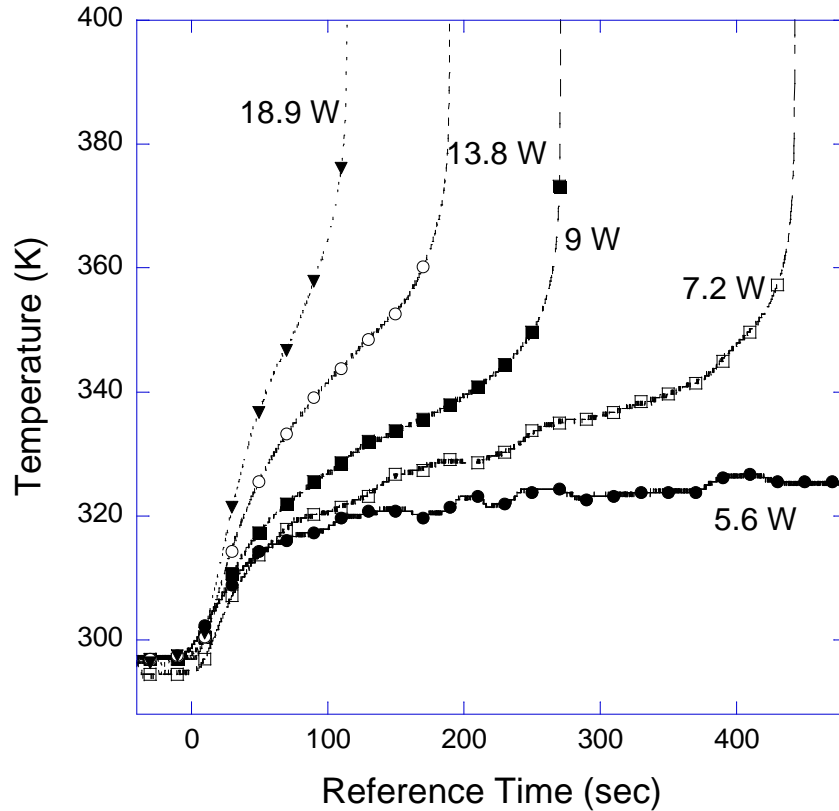


Figure 7: Comparison of temperature histories with varying power inputs. Inlet conditions $\Phi = 0.4$ and $k = 400 \text{ s}^{-1}$.

3.1.1.2 Transition to a Gas-Phase Flame

Figure 8 demonstrates the possibility of transition from catalytic surface reactions to a gas-phase flame. For this case ($\Phi = 0.4$ and $k = 100 \text{ s}^{-1}$), the surface is initially held at a temperature above the catalytic ignition temperature T_C using electrical heat input. When the H_2/air pre-mixture is impinged on the surface, catalytic ignition is observed as shown. Once the surface temperature has reached its new steady-state, more power is applied to the heater to further increase the surface temperature. As the heat input reaches a critical point, a gas-phase flame emerges, indicated in Fig. 8 by a large spike in surface

temperature around $t = 750$ s. Once another steady-state surface temperature is reached, the heater power is shut off, which in this case results in a noticeable surface temperature drop. Despite this drop, a steady-state flame is retained. Following hydrogen shutoff similar to the previously described catalytic case, typical exponential cooling is evident after the flame extinguishes. In addition, it has been observed for some overpowered cases, which have the initial heat input higher than the minimum value necessary for catalytic ignition, that no additional heat input is necessary, and that a gas-phase ignition can occur directly from the heat released as a result of catalytic reactions.

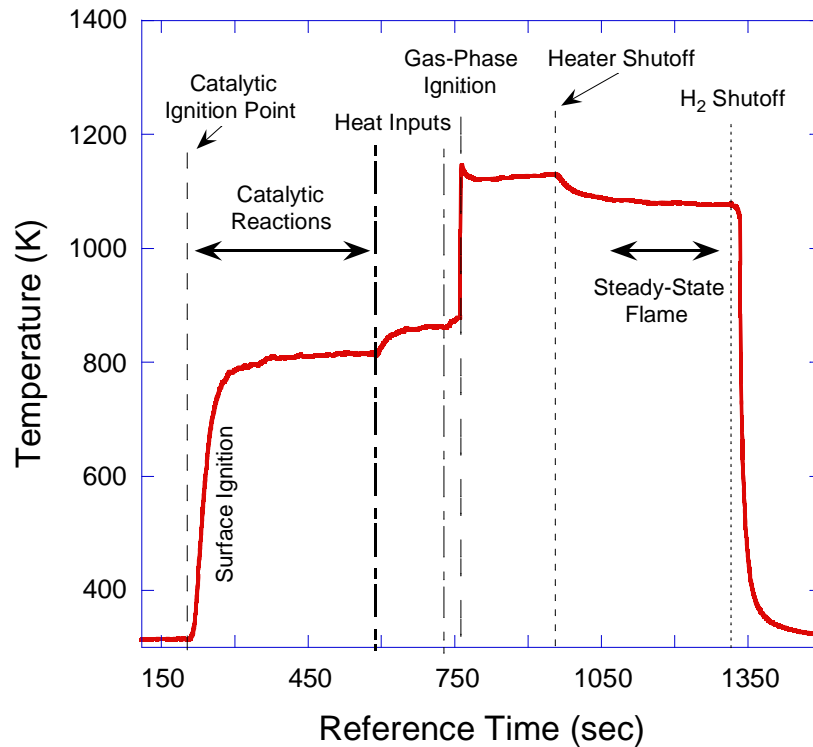


Figure 8: Demonstration of catalytic activity transitioning to a gas-phase flame. Inlet conditions $\Phi = 0.4$ and $k = 100 \text{ s}^{-1}$.

Despite the ability for the experimental system to develop gas-phase flames based upon heat release from catalytic reactions, the transition between the two modes has not

been observed to occur at consistent temperatures. Should the platinum foil within the stagnation plate change shape slightly (i.e. some wrinkling of the surface is noted as a result of thermal cycling), it has been qualitatively observed that this can drastically change the temperature at which a transition occurs. These observations suggest that gas-phase ignition for a hot, catalytic surface is largely controlled by the nature of heat transfer into the impinging gas flow. This transition may be further complicated by kinetic and diffusion effects that have been previously discussed in the literature, namely that gas-phase ignition can be inhibited by H-radical termination reactions at the platinum surface. As a result, the critical temperature for gas-phase flame transition is not further investigated experimentally in this work.

3.1.1.3 Catalytic Ignition Temperature Variation with Equivalence Ratio

Figure 9 shows the variation in catalytic ignition temperature with equivalence ratio for $k = 300 \text{ s}^{-1}$. It is found that for equivalence ratios in an ultra-lean regime ($\Phi = 0.2$ and below), catalytic ignition requires no external heating and the flow of H_2/air mixtures against the platinum surface leads directly to thermal runaway. Certain cases (not shown for clarity) have been examined down to $\Phi = 0.05$ and show that ignition continues to occur at room temperature. As equivalence ratio increases above $\Phi = 0.2$, T_C increases abruptly from room temperature to a maximum of $\sim 365 \text{ K}$ near $\Phi = 0.4$ and remains essentially constant as equivalence ratio increases further towards the stoichiometric condition. As such, it appears that two ignition regimes may exist; room temperature ignition and elevated ($\sim 365 \text{ K}$) temperature regimes separated by an abrupt transition between $\Phi = 0.2$ and 0.3 .

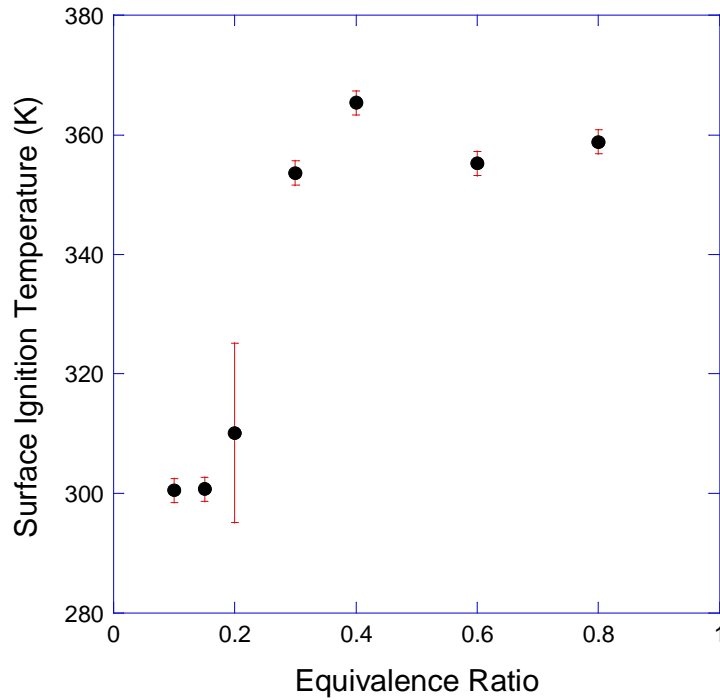


Figure 9: Experimental catalytic ignition temperatures for varying inlet equivalence ratio conditions with constant stretch rate of $k = 300 \text{ s}^{-1}$.

It should also be noted that for the $\Phi = 0.2$ case, a relatively larger scatter is observed. Uncertainty in T_C measurements is estimated in this experiment through the standard deviation for all tests conducted for each data point. While for most cases this uncertainty remains within $\sim 3 \text{ K}$, $\Phi = 0.2$ represents what could be termed a transition region between room temperature and elevated temperature ignition regimes. While for most of $\Phi = 0.2$ cases catalytic ignition occurs at room temperature, a small percentage of experiments require heating to $\sim 330 \text{ K}$. This variability is presumed to be the result of hysteresis effects on the platinum foil coupled with an increased sensitivity to equivalence ratio variation in this operation region. Similar variability prevented data collection within the region between $\Phi = 0.2$ and 0.3 , as the presumed coupling effects rendered any average value of T_C meaningless. Therefore, while the existence of this

transition region is apparent based upon the available data, further resolution of ignition properties within it is not possible using the current apparatus, and may be impractical due to the combined effects of catalyst hysteresis and sensitivity. However, for the purposes of fire safety, the transition between room temperature and elevated temperature ignition regimes represents a change of only 60–70 K, a result that may not significantly change how a hazard is evaluated.

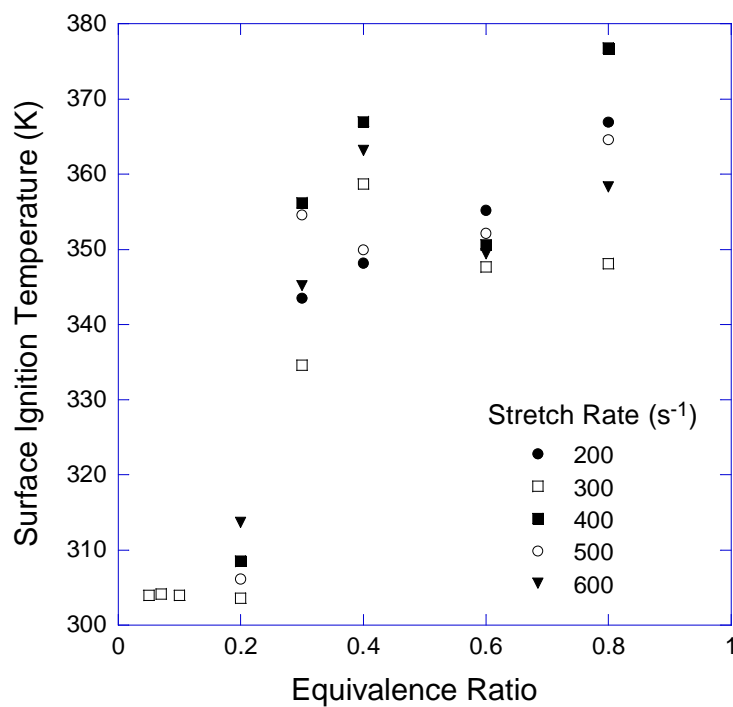


Figure 10: Comparison of the effect of equivalence ratio for varying stretch rate conditions between $k = 200$ and 600 s^{-1} .

Additional catalytic ignition data has been collected for varying equivalence ratios with a range of stretch rates over a platinum stagnation surface. As demonstrated in Fig. 10, the trends observed for $k = 300 \text{ s}^{-1}$ shown in Fig. 9 are largely retained for varied stretch rate conditions. For $k > 300 \text{ s}^{-1}$, room temperature ignition is again observed for $\Phi = 0.2$ (within uncertainty), and exhibits similar increases in T_C to between 350 and 370 K

for $\Phi > 0.2$. In addition, the plateau behavior is largely preserved across all stretch rates between $\Phi = 0.4$ and 0.8. This suggests that the relationship between T_C and equivalence ratio does not change significantly as stretch rate increases. Figure 10 additionally suggests that equivalence ratio may be the dominant factor in determining catalytic ignition temperature, as all stretch rates tested appear to follow similar trends across the experimental range.

3.1.1.4 Catalytic Ignition Temperature Variation with Stretch Rate

Based upon the results of Fig. 10, it could be argued that the response of the platinum surface does not change significantly within a range of flow conditions. To observe whether this is the case, catalytic ignition temperatures are studied for $\Phi = 0.4$ (representing the beginning of the plateau in ignition temperatures mentioned previously) over a much wider range of stretch rates for $k = 100\text{--}1200\text{ s}^{-1}$. The dependence of T_C on stretch rate is plotted in Fig. 11.

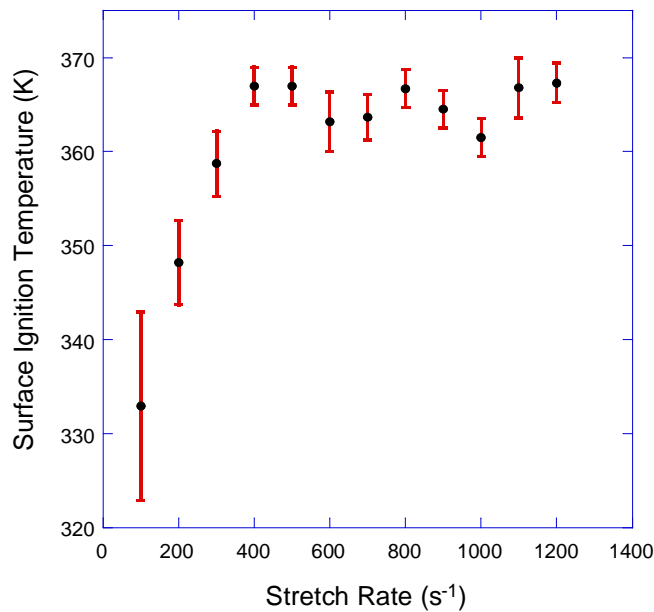


Figure 11: Catalytic ignition temperature variation with stretch rate for $\Phi = 0.4$.

It is observed that surface ignition temperatures increase by ~ 35 K between $k = 100$ and 400 s^{-1} , and remain approximately within experimental error throughout the remainder of the experimental range. Although increased stretch rate is seen to increase the observed surface ignition temperature for $k < 400 \text{ s}^{-1}$, above this threshold stretch rate value no discernable variation in T_C can be observed, even as stretch rate is increased by a factor of three. While the experimental apparatus does not allow for further reduction in stretch rate below $k = 100 \text{ s}^{-1}$, the trend in Fig. 11 also suggests a progression towards room temperature as stretch rate is reduced.

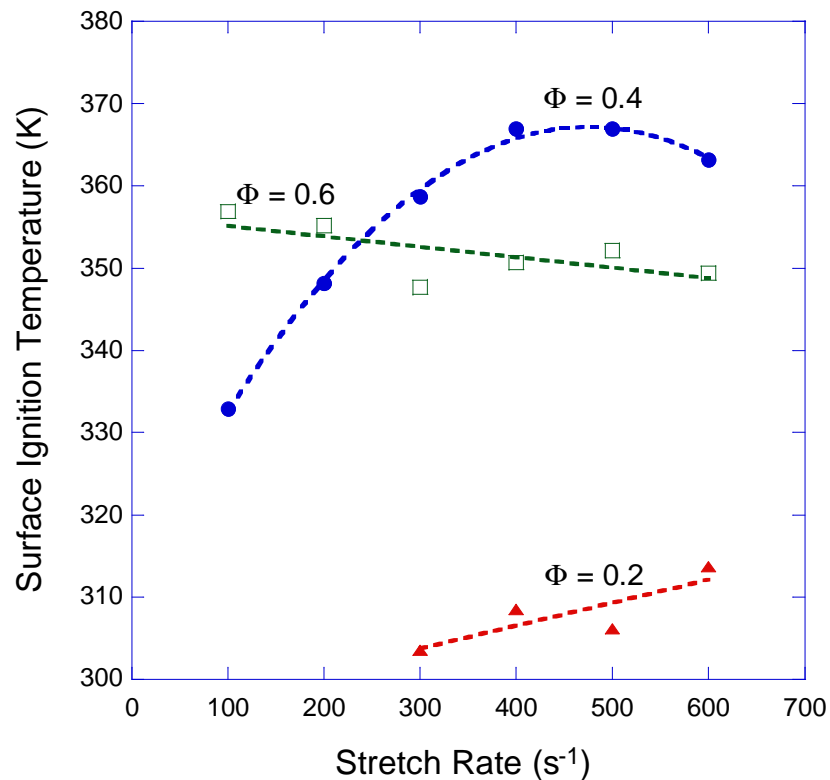


Figure 12: Comparison of the effect of stretch rate variation on surface ignition temperature for various equivalence ratios.

The preceding discussion has been focused upon the single equivalence ratio of $\Phi = 0.4$. Figure 12 presents the stretch rate dependence results for $\Phi = 0.2$ and 0.6 and over

a stretch rate range of $k = 100\text{--}600 \text{ s}^{-1}$. As is evident, the trends observed for $\Phi = 0.4$ do not extend to other equivalence ratios, as the $\Phi = 0.2$ case exhibits near-room-temperature T_C and the $\Phi = 0.6$ case remains nearly constant across the range of stretch rates. This behavior provides additional support for the aforementioned hypothesis that equivalence ratio is the dominant factor determining the catalytic ignition temperature for given operating conditions.

3.1.1.5 Steady-State Post-Ignition Surface Temperature

Thus far, we have focused our attention on the ignition properties of H_2/air mixtures over a platinum surface. Ultimately, however, the steady-state post-ignition temperatures achieved on the catalytic surface are also of great importance to any hazard evaluation. As such, Fig. 13 shows the variation in steady-state surface temperature for $\Phi = 0.2\text{--}0.8$ with $k = 300 \text{ s}^{-1}$ after catalytic ignition. Even for equivalence ratios as low as 0.2, steady-state surface temperatures can reach as high as 900 K, enough to melt or soften most aluminum alloys. This post-ignition surface temperature increases to a maximum of 1200 K near $\Phi = 0.5$, and remains relatively constant thereafter. The observation that this achieved surface temperature does not continue to rise with increasing equivalence ratio towards stoichiometric suggests that a preferential equivalence ratio may exist near $\Phi = 0.4\text{--}0.5$; an interesting result considering the plateau in catalytic ignition temperatures begin in the same region, as shown earlier.

To further explore the unique response near $\Phi = 0.4\text{--}0.5$, additional comparisons are made for the thermal runaway profiles for $\Phi = 0.2\text{--}0.8$ with $k = 400 \text{ s}^{-1}$. For these experiments, the surface temperature is raised to a point where thermal runaway would

occur spontaneously upon exposure to the H₂/air mixture in question. While heat input values are not identical in all cases, previous results (not shown) have not observed any variation in the nature of thermal runaway with the range of heat inputs used here. It can be seen in Fig. 14 that as equivalence ratio increases from $\Phi = 0.2$ to 0.4, the temperature begins to rise towards a steady state significantly faster. However, as equivalence ratio is increased further, this rising rate begins to drop towards previous levels (i.e. $\Phi = 0.2$ and 0.8 exhibit similar rising rates, while $\Phi = 0.3$ and 0.6 are practically identical). This result provides further substantiation for a preferential equivalence ratio near $\Phi = 0.4$ –0.5 for catalytic reactivity.

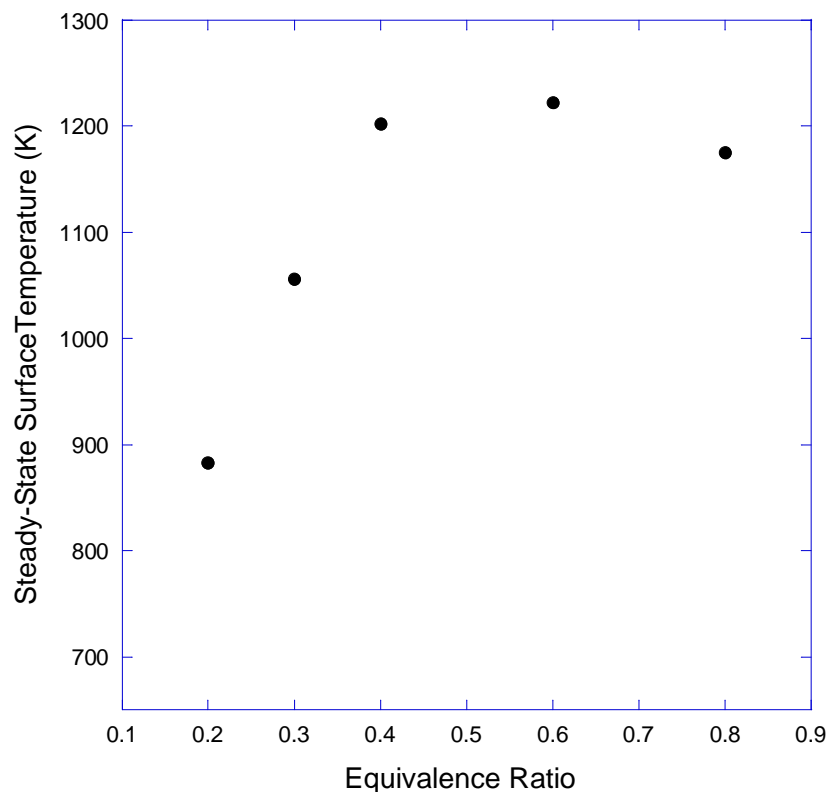


Figure 13: Comparison of steady-state post-ignition surface temperatures at varying equivalence ratios for a stretch rate of $k = 300 \text{ s}^{-1}$.

It is worth noting that the steady-state surface temperatures achieved on the platinum

surface are the result of a balance between the chemical energy release of H₂/air at the platinum surface, heat conduction to the ceramic material, and heat convection to the gas flow. Since the nature of the heat transport is unique to the shape, size, and materials used for the stagnation assembly, the results presented in this section may provide only a qualitative measure of chemical energy release. Despite the qualitative nature of these results, the trends suggest that achievable post-catalytic-ignition surface temperatures can reach well into regions where gas-phase ignition has been observed, and structural damage or failure may occur via melting, softening, or enhanced oxidation.

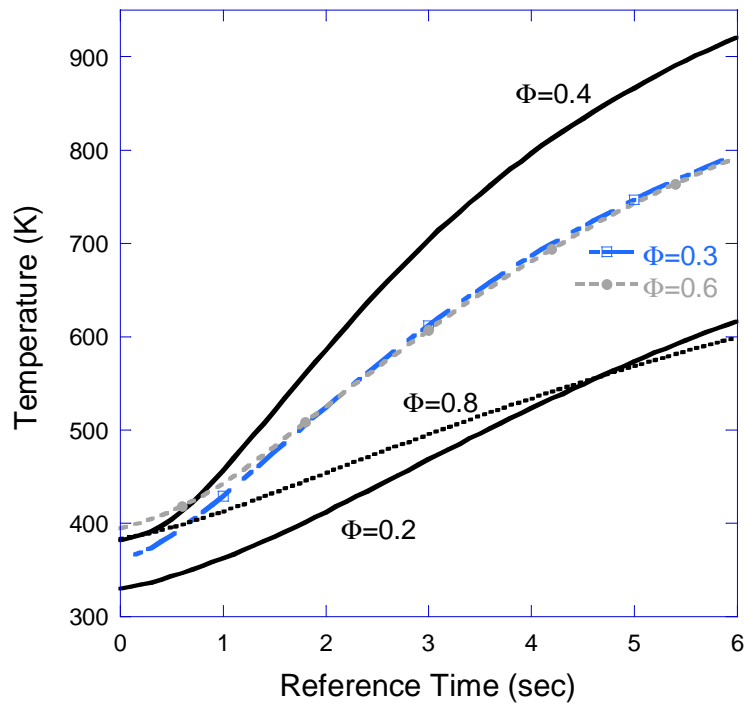


Figure 14: Comparison of the rising rate of surface temperature evolution profiles for varying equivalence ratios and stretch rate $k = 400 \text{ s}^{-1}$. It is seen that rising rate reaches a maximum near $\Phi = 0.4$ before falling back to a slower rate as equivalence ratio continues to increase.

3.1.1.6 Morphological Effect on Surface Reactivity

Across all experiments shown previously, a single platinum foil is used for consistency.

However, it has been observed that morphological changes in the foil have occurred with continued usage. Figure 15 shows X-Ray diffraction patterns for two available platinum foils; the high-activity foil which is used here, and a low-activity foil from the same lot.

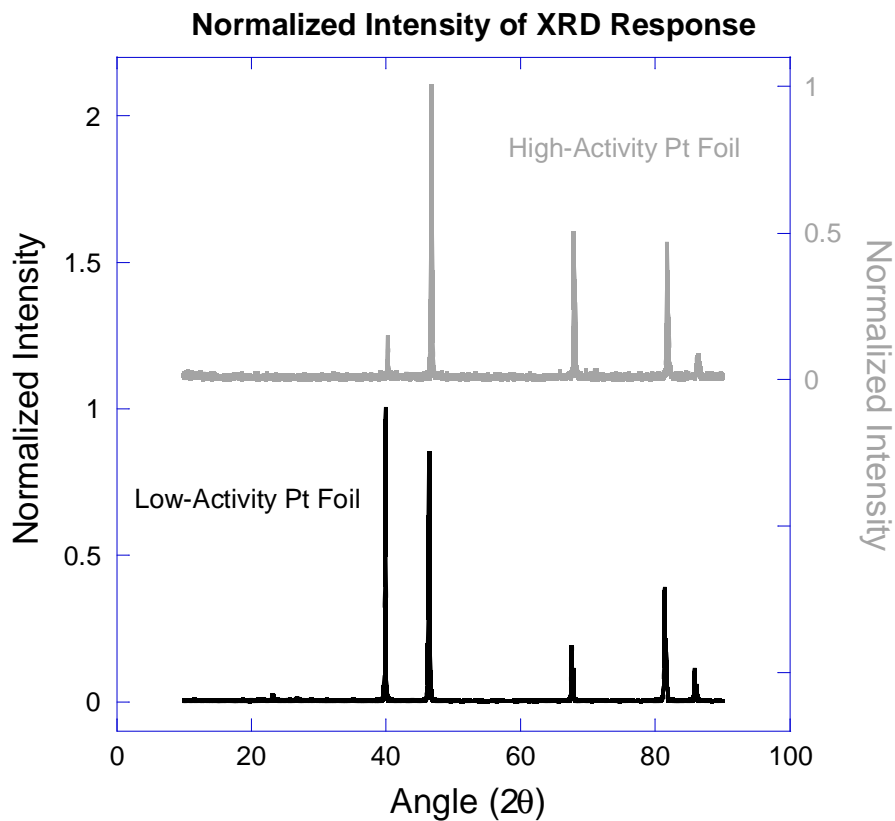


Figure 15: X-Ray Diffraction patterns for the high-activity platinum foil used in this study as compared to a low-activity foil from the same manufacturer and lot.

It can be seen that while the position of the peaks typical of a platinum sample remain the same in both foils, the high-activity foil varies significantly in the relative intensity of several peaks, suggesting that structural changes have occurred within the foil. While the exact nature and cause of these differences is currently unknown, they result in a reduction (relative to the low-activity foil) of catalytic ignition temperatures by approximately 40 K. Such changes have been noted before in the literature, noting that

morphological changes of a platinum surface have led to variations in product selectivity. Such changes have been attributed to thermal cycling. However, for the purposes of fire safety, the overall behavior in terms of ignition properties do not change substantially and the surface ignition temperature variation of 40 K does not significantly change the nature of any hazard posed by a catalytic surface.

3.1.2 Common Metal and Metal-Oxide Experiments

The following sections describe the results obtained from the stagnation-plate assembly utilizing common metal and metal-oxide foils in place of the platinum foil. For all tested materials, the stagnation plate is constructed using metallic foils that are allowed to naturally oxidize as a result of testing. This is done considering that testing of a pure metal cannot be conducted due to rapid or immediate surface oxidation as a result of exposure to air. The choices of metals for testing are then based upon typical materials that may be found as pure metals or major constituents of alloys or coatings.

While only a single stretch rate condition is presented here, additional investigation has been conducted at additional stretch rates. However, as additional stretch rates result in identical conclusions, no further testing is deemed necessary.

3.1.2.1 Aluminum

Aluminum is a widely used lightweight structural material that may be found in a variety of products that might be found in a typical garage setting. Due to aluminum spontaneously forming a protective oxide upon exposure to air, no apparent oxidation is observed during testing.

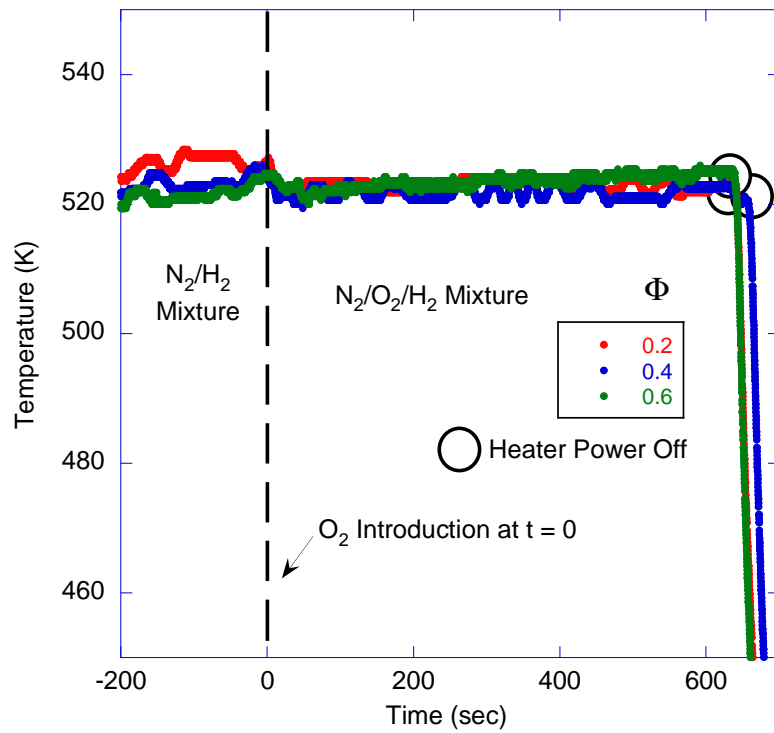


Figure 16: Evaluation of surface reactivity for an aluminum stagnation surface. Stretch rate $k = 200 \text{ s}^{-1}$.

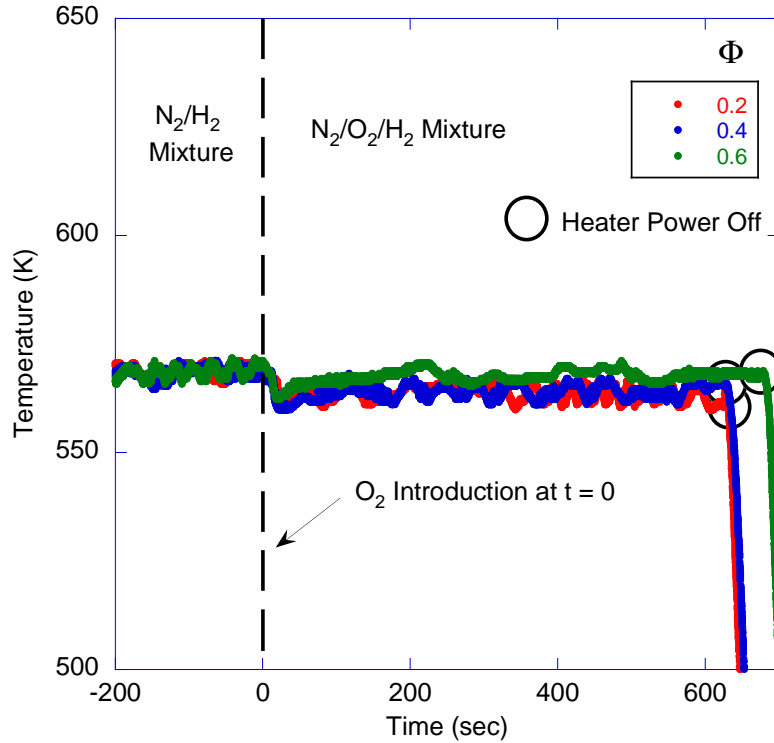


Figure 17: Evaluation of surface reactivity for an iron stagnation surface. Stretch rate $k = 200 \text{ s}^{-1}$.

Figure 16 shows the results for three equivalence ratios tested at the maximum heater-imposed temperature for the aluminum stagnation plate for a stretch rate of $k = 200 \text{ s}^{-1}$. At time $t = 0$, an N_2/H_2 mixture at the given stretch rate is replaced with an $\text{N}_2/\text{O}_2/\text{H}_2$ mixture. Initially, the temperature is steady at approximately 520 K. Following $t = 0$, a slight drop in surface temperature is observed as a result of transient flow as a result of flow switching. Should there be any surface reactivity that would suggest exothermic reactions, a temperature rise similar in nature to that observed for a platinum surface would be expected. As demonstrated in Fig. 16, no such temperature rise is observed, and upon heater shutoff the surface exhibits immediate cooling behavior that replicates that observed for a non-reactive mixture, indicating that for these conditions no large-scale exothermic reactions occur. In addition, no apparent damage or oxidation occurs during testing. Taken together, these results do not suggest any catalytic activity or other surface reactions occurring on the aluminum foil. Based upon this data, no apparent fire safety hazard is observed up to the maximum temperature achievable, in this case $\sim 520 \text{ K}$.

3.1.2.2 Iron

Iron is of interest as it forms the basis for most common structural materials, i.e. steel. As a result, there are numerous opportunities for leaked hydrogen to come into contact with iron or its oxides under normal conditions.

Figure 17 shows the results from identical flow conditions as were tested for the aluminum stagnation plate, i.e. $k = 200 \text{ s}^{-1}$. For this stagnation plate, the maximum temperature achieved is $\sim 570 \text{ K}$. As with the previous case, at time $t = 0$ the non-reactive

N₂/H₂ mixture is replaced with a reactive N₂/O₂/H₂ mixture, resulting in a slight surface temperature drop. After a period of approximately 10 minutes, the surface temperature remains steady at the $t < 0$ temperature, proceeding directly to room temperature following heater power shutoff. As with the aluminum tests, this behavior suggests no catalytic reactions proceeding on the iron surface.

Unlike the aluminum surface, iron quickly exhibited significant surface condition changes during testing, the result being significant surface oxidation in the form of an adherent black scale. The deviation from the original condition indicates that the surface is primarily an iron oxide during testing. While this may not be a realistic situation for the case of an alloy, on a micro-scale any iron at a free surface could be expected to form a small patch of an iron oxide, and alloying behavior is not expected to drastically change the behavior of an otherwise non-reactive substance.

3.1.2.3 Zinc

Zinc is of interest as a result of its common use as a coating material for steels through the galvanizing process, most prominently for automotive steel. These applications suggest that any potential activity in conjunction with hydrogen/air mixtures deserves investigation.

Figure 18 shows the results from testing under conditions identical to the two previous cases. As before, no reactivity is evident up to the maximum temperature for this stagnation plate (~580 K). No oxidation was apparent after testing had been completed.

3.1.2.4 Nickel

Nickel is of particular interest as a result of its location on the periodic table, namely above the platinic group which includes several highly active hydrogen catalysts. In addition, nickel is used as a low-cost catalyst in several processes, including the production of hydrogen via various reforming methods. It may also be present in a typical consumer setting as a result of its common usage as a plating material for the purposes of wear resistance and corrosion protection.

Figure 19 shows the results obtained for a nickel stagnation surface for stretch rate $k = 200 \text{ s}^{-1}$. Once again, up to the maximum temperature of $\sim 560 \text{ K}$, no apparent exothermic reactions are observed on the stagnation surface, suggesting that the nickel surface does not serve as a highly active catalyst for H_2/air mixtures. In consideration of nickel being the most likely of the listed candidates to exhibit catalytic activity, despite these negative results in a stagnation configuration, additional testing is conducted in the microtube configuration, which will be described in Section 3.2.3.

3.1.2.5 Copper

Though initially considered for testing, copper has a well-known reduction/oxidation pathway with hydrogen and oxygen. As a result, no detailed testing is conducted.

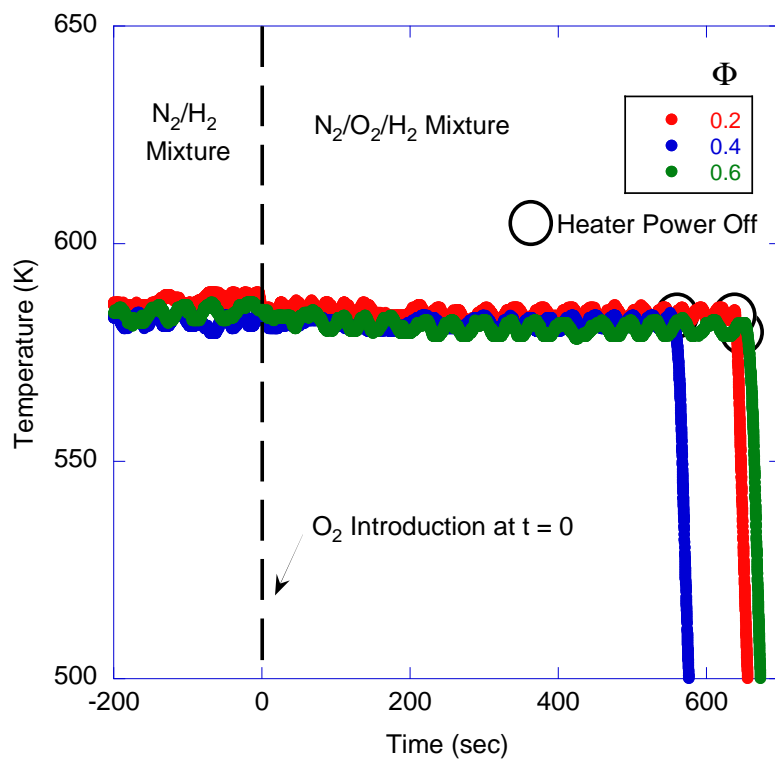


Figure 18: Evaluation of surface reactivity for a zinc stagnation surface. Stretch rate $k = 200 \text{ s}^{-1}$.

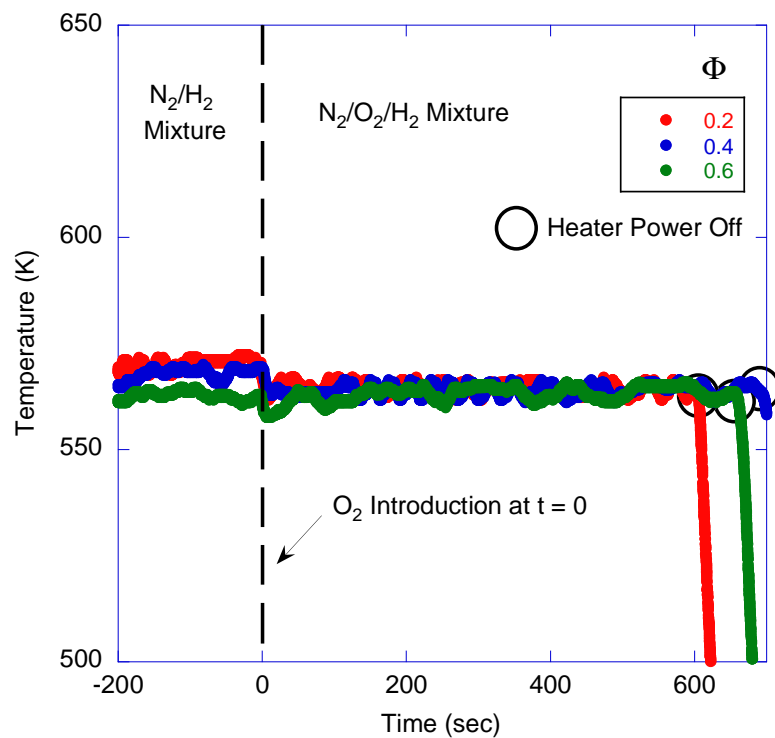


Figure 19: Evaluation of surface reactivity for an iron stagnation surface. Stretch rate $k = 200 \text{ s}^{-1}$.

3.2 Catalytic Microtube Experiment

3.2.1 0.8 mm Platinum Tube

The tubular configuration provides an experimental advantage over the stagnation-point flow by virtue of being able to provide very low flow velocities over the platinum surface, allowing test conditions that would otherwise be inaccessible. In order to better compare these results to those obtained from the stagnation-point flow configuration, the quantity of “equivalent stretch rate” is quoted for each case. Here, equivalent stretch rate is defined as the inverse of the residence time through the heated length of the tube. As a result, temperature response can be investigated as a function of both flow velocity/residence time and equivalence ratio.

Shown in Fig. 20 is a typical temperature response for a non-reactive flow with a mixture equivalent to $\Phi = 0.8$, with an inlet velocity of 4.5 m/s or an equivalent stretch rate of $k = 32.12 \text{ s}^{-1}$. As would be the case in the stagnation-point flow configuration, a non-reactive flow is created by replacing the oxygen in the air fraction of the mixture with additional nitrogen. When reactions do not occur within the tube, it is observed that TC1, the location nearest the inlet of the tube, exhibits the lowest temperature, while TC2 and TC3 are nearly identical at a slightly higher temperature. Additionally, the temperature settles at essentially steady-state within approximately one minute. Finally, when the external heat input is removed the temperature of all three thermocouples drops immediately to room temperature within approximately 20 seconds. This behavior serves as a baseline so that ignition can be readily defined.

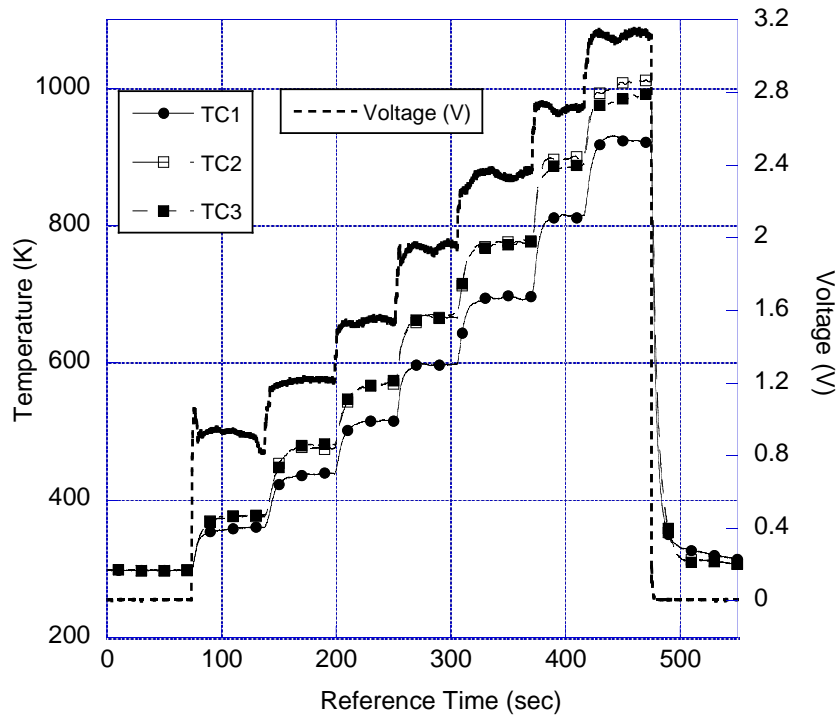


Figure 20: Characteristic response for N_2/H_2 at H_2 flow equivalent to $\Phi = 0.8$. N_2 replaces O_2 at a rate commensurate with an inlet velocity of 4.5 m/s or equivalent stretch rate $k = 32.14 \text{ s}^{-1}$.

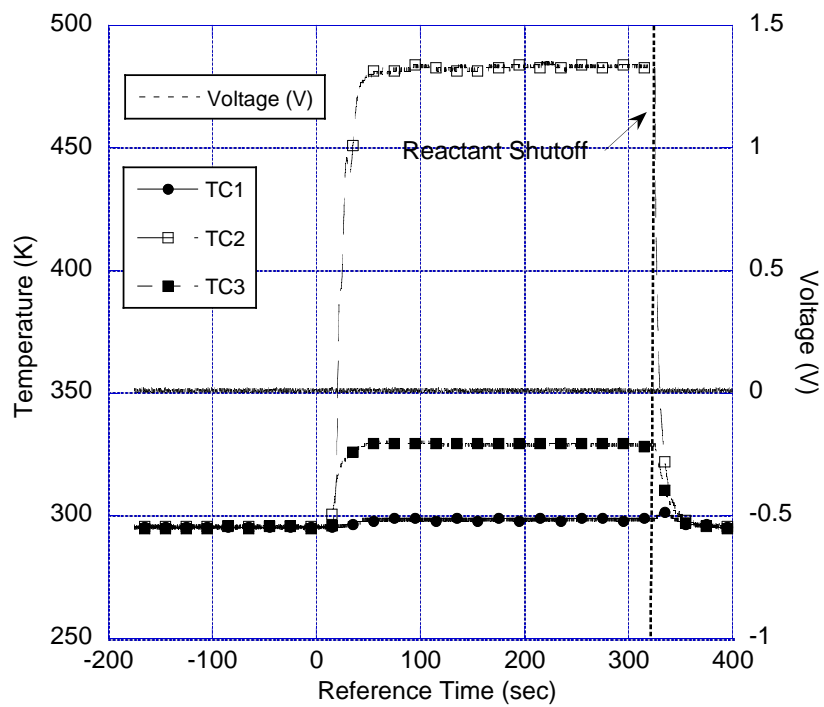


Figure 21: Characteristic response for H_2/Air at $\Phi = 0.2$ and inlet velocity of 4 m/s or $k = 28.57 \text{ s}^{-1}$.

Figure 21 exhibits behavior characteristic of catalytic ignition within the 0.8 mm diameter platinum tube, for conditions of $\Phi = 0.2$, and an inlet velocity of 4 m/s, corresponding to $k = 28.57 \text{ s}^{-1}$. From room temperature and with no power applied across the tube, the tube temperature at TC 2 rises to $\sim 480 \text{ K}$, while TC3 experiences a much lower rise, and TC1 is essentially unaffected. This behavior suggests that a reaction zone in the tube is located nearest TC2. The fact that these reactions proceed directly from room temperature is interesting in the context of the stagnation-point flow experiments, as it was observed that as global stretch rate was reduced towards zero, the catalytic ignition temperature seemed to proceed towards room temperature. In contrast to this behavior, Fig. 22 shows the characteristic response for $\Phi = 0.2$ at a lower inlet velocity of 2 m/s ($k = 14.28 \text{ s}^{-1}$). While room temperature ignition is still observed, TC 2 exhibits a sawtooth-type temperature response, suggestive of a cyclic process balancing reaction rate and a reactant deficit in the reaction zone. This is further supported by a case with further reduced flow rate, shown in Fig. 23, where power must be applied to the tube in order to observe a limited temperature response near TC1, which does not self-sustain following power shutoff. Similar results are obtained for equivalence ratios up to $\Phi = 0.8$, with the exception of $\Phi = 0.4$. Taken together, these observations suggest that a minimum flow rate of reactants to the catalytic surface is necessary to observe room temperature ignition, as the ignition event cannot self-sustain without sufficient energy input from additional reactants. In addition, the deviation from typical behavior at $\Phi = 0.4$ further suggests – when considered in conjunction with the behavior observed in the stagnation-point flow experiment at the same conditions – that this mixture represents a special case, though why this might be true is currently unclear.

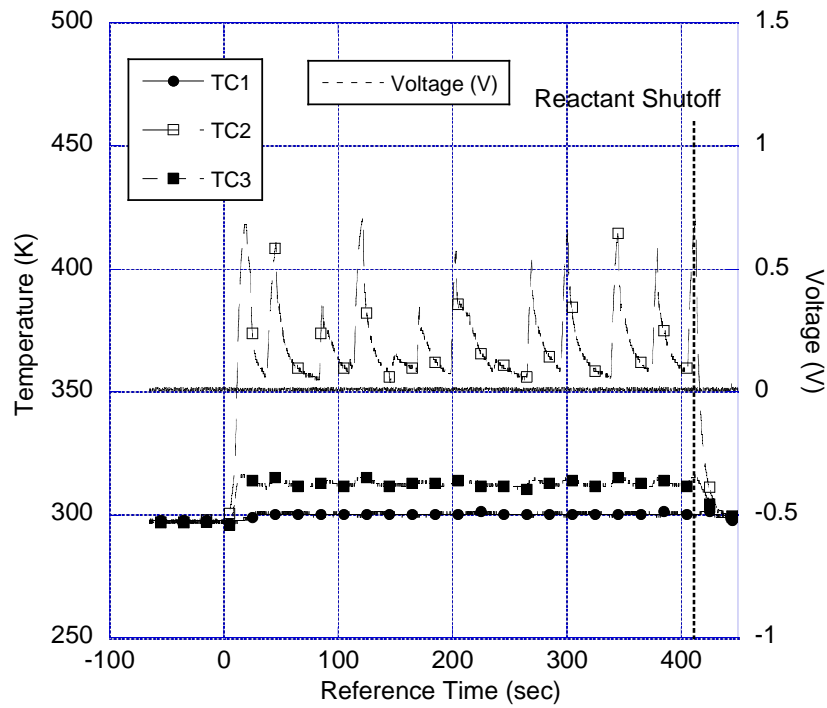


Figure 22: Characteristic response for H₂/Air at $\Phi = 0.2$ and inlet velocity of 2 m/s or $k = 14.28 \text{ s}^{-1}$.

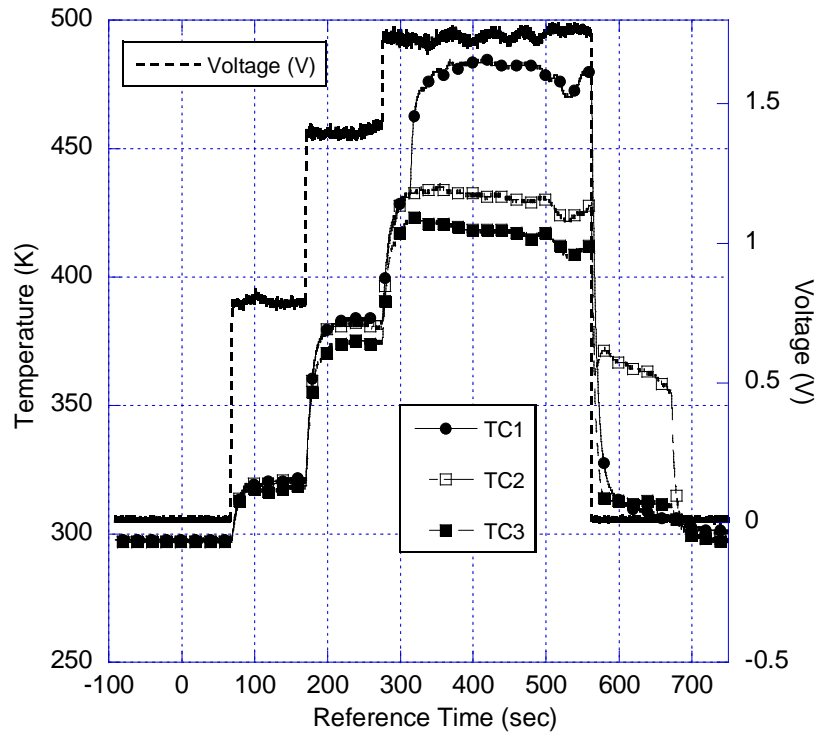


Figure 23: Characteristic response for H₂/Air at $\Phi = 0.2$ and inlet velocity of $\dot{}$ m/s or $k = 7.14 \text{ s}^{-1}$.

Additional materials not discussed here are compiled using this experiment, and are further discussed in the master's thesis entitled, "Ignition Propensity of Hydrogen/Air Mixtures in the Presence of Heated Platinum Surfaces." This work is available upon request, or is publicly available at etd.ohiolink.edu.

3.2.2 *0.4 mm Platinum Tube*

As previously mentioned, the intent behind the use of two varying tube diameters is to determine how geometrical conditions may impact the ignition properties of the H₂/air system on a platinum surface. However, despite the similarity between the configurations, the results observed in this configuration depart significantly from those observed in the larger diameter case. Whereas at many equivalence ratio and flow velocity combinations the 0.8 mm diameter tube exhibited catalytic ignition at room temperature, for no case was room temperature ignition observed for the 0.4 mm diameter tube. In fact, all cases observed exhibit catalytic ignition at surface temperatures greater than 100 K above room temperature. However, primarily as a result of the low mass of the experimental section in combination with the relatively high heat loss due to high surface area-to-volume ratio, significant variability is present in the data, and prevents a meaningful comparison with previous experiments.

3.2.3 *0.4 mm Nickel Tube*

As mentioned in Section 3.1.2.4, nickel is considered a prime candidate for potential catalytic activity as a result of its usage as a reforming catalyst. To further investigate this possibility, a 0.4 mm diameter tube is used to help determine what if any activity is

observed. Figure 24 shows a typical temperature response for this configuration. Shown in blue, the non-reactive H_2/N_2 temperature and voltage histories illustrate that as the power is increased to the tube, temperature increases in a step-wise fashion. Only the results of a single thermocouple are shown for the sake of clarity. However, for a reactive H_2/air case under the same conditions a deviation from this behavior can be observed as the surface temperature passes 1000 K. Whereas at a slightly higher power input the non-reactive case remains at ~ 1100 K, the reactive case exhibits exothermic behavior which elevated the surface temperature near TC2 to just above 1200 K. However, considering the surface temperature at which this behavior occurs, it is unclear whether it is the result of surface activity or simply a gas-phase reaction supported by external heat input. In addition, given the extremely high temperatures where exothermicity is observed, it is unlikely that these conditions would be applicable to a fire safety scenario.

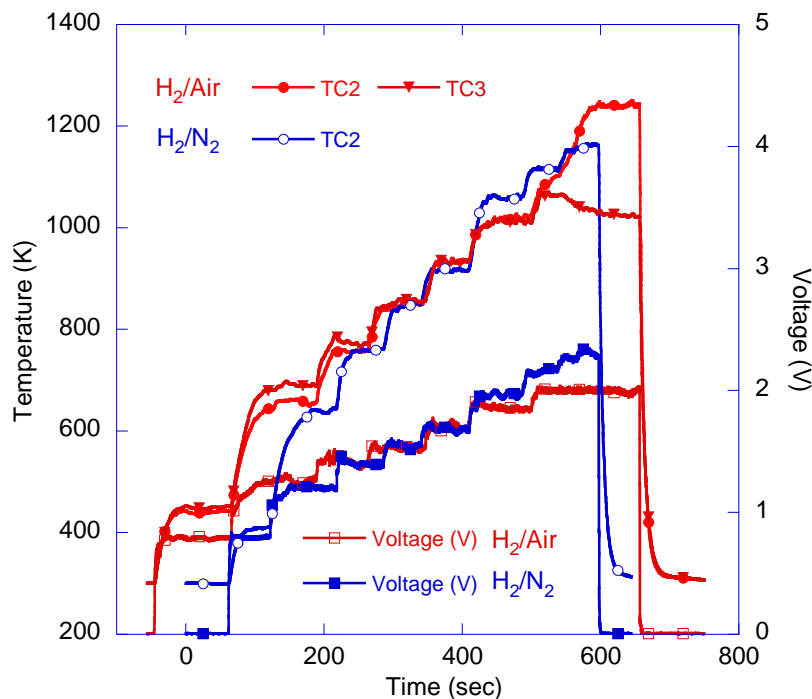


Figure 24: Typical temperature history for a 0.4 mm diameter nickel tube, showing both reactive and non-reactive temperature/voltage histories for $\Phi = 0.8$ and inlet velocity of 18 m/s.

3.3 Scaled Garage Experiment

As described in Section 2.3, the scaled garage experiment represents a 1/16th scale two-car garage. Of particular interest are the typical response of a catalyst at various positions, the hydrogen concentrations that evolve, and the impact of various venting scenarios. As such, two sets of data are collected for each condition tested, including surface temperature data from the catalyst and hydrogen concentration data at four elevations within the garage. For all cases described here, the topmost sensor is labeled as Sensor 1, while the bottommost is labeled as Sensor 4. In Sections 3.3.1 and 3.3.2, the venting condition used for all testing is two 0.25 inch diameter holes in the garage wall. The top hole is located 1 inch from the roof and 0.75 inch from the corner, while the bottom hole is located 0.75 inch from the floor and the corner. Additional configurations are discussed in Section 3.3.3.

3.3.1 Characteristic Temperature and Hydrogen Measurements

In order to better facilitate comparison of the current experiment to the results of the stagnation-point flow experiment, experiments are conducted within the scaled garage using a premixed inlet condition in the equivalence ratio range of $\Phi = 0.2$ – 0.8 . Figure 25 shows a characteristic response for an inlet condition of $\Phi = 0.6$ at a flow rate of 0.1 g/s. For this test, the catalyst is located 11.5 cm above the garage floor, 9 cm horizontally offset from the inlet and facing downwards. Shortly following the introduction of the mixture to the system (seen as a rise in hydrogen concentration) the surface temperature begins to rise from its initial value near 300 K, reaching a steady-state temperature of ~675 K and a steady hydrogen concentration slightly below $\Phi = 0.6$. This slight deviation

from the inlet mixture is expected as a result of vents allowing outside air to enter the chamber, as well as hydrogen consumption by the catalyst surface. Although it is generally anticipated that even for a premixed condition the hydrogen within the garage will stratify to a certain extent, no appreciable stratification is indicated by the sensors.

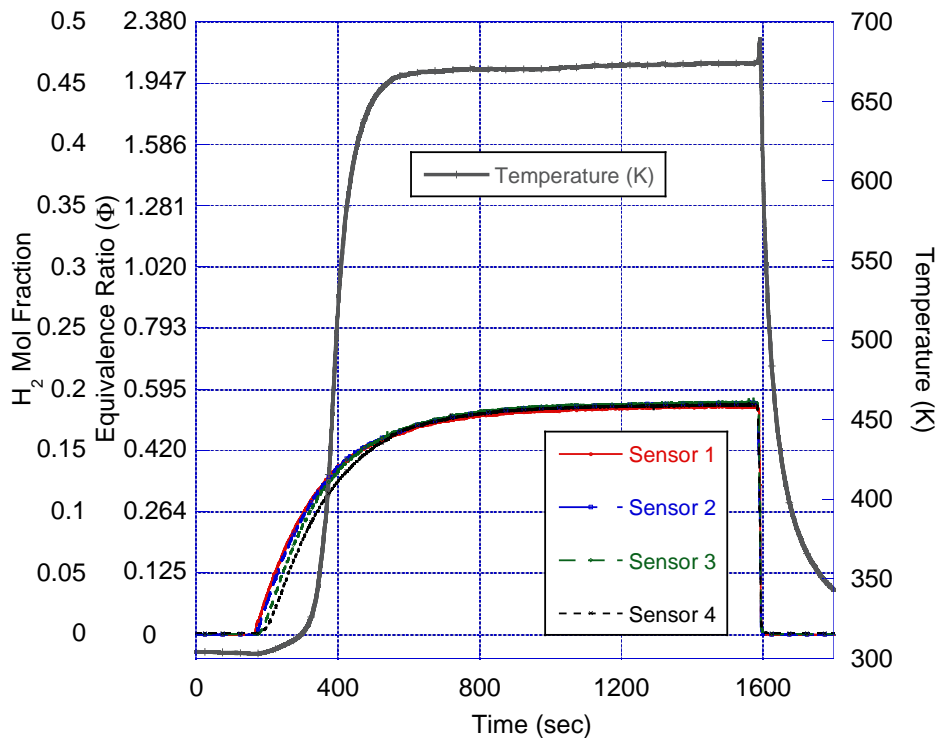


Figure 25: Characteristic temperature and hydrogen concentration response for $\Phi = 0.6$ at a flow rate of 0.1 g/s. Catalyst is located 11.5 cm above the garage floor, 9 cm offset from the inlet.

Despite some initial separation amongst the measurements – initial observation of hydrogen proceeds progressively from the topmost to bottommost sensor – at steady state all measurements converge to the same value. Two potential causes may explain this behavior. The relatively higher flow rate associated with a premixed flow (0.1 g/s) may cause a small degree of convective mixing to occur. However, given the low velocity of the flow exiting the diffusing inlet, this type of mixing should be minimal. More likely,

the incoming hydrogen/air mixture is provided to the garage at a rate that is greatly in excess of the rate at which reactants naturally diffuse through vents in the garage walls, which results in the mixture in the garage largely retaining the properties of the premixed flow.

In comparison, Fig. 26 shows a typical response for a hydrogen-only inlet flow rate of 0.0015 g/s H₂. Whereas for a premixed inlet condition hydrogen concentration is essentially independent of height within the garage, for the hydrogen-only inlet condition the mixture within the garage is highly stratified, for this case exhibiting a difference of ~7% between the highest and lowest measurement heights with concentration increasing monotonically as height increases. In addition, whereas for the premixed case the mixture ratio within the garage is determined by the inlet mixture, for the hydrogen-only inlet condition the mixture becomes highly fuel-rich as time progresses, with the ultimate steady-state value determined by the inlet flow rate (discussed further in Section 3.3.3). In addition to the differences in measured hydrogen concentration, the surface temperature response observed as a result of a pure hydrogen flow varies significantly from the premixed results. While in the case of premixed inlet condition the temperature rises to a steady-state and remains at that level until the garage is vented, a pure hydrogen flow results in a peak in temperature after ignition, followed by a slow decline as the experiment continues and hydrogen concentration continues to build throughout the garage. The major difference between these cases is of course the hydrogen concentration, which remains below $\Phi = 1$ for all premixed cases, but which readily exceeds stoichiometric when the inlet flow is hydrogen-only. From a fire-safety perspective, this

suggests that for a catalytic ignition source, an ideal hydrogen flow rate should exist that maintains a “preferred” equivalence ratio that maximizes the surface temperature.

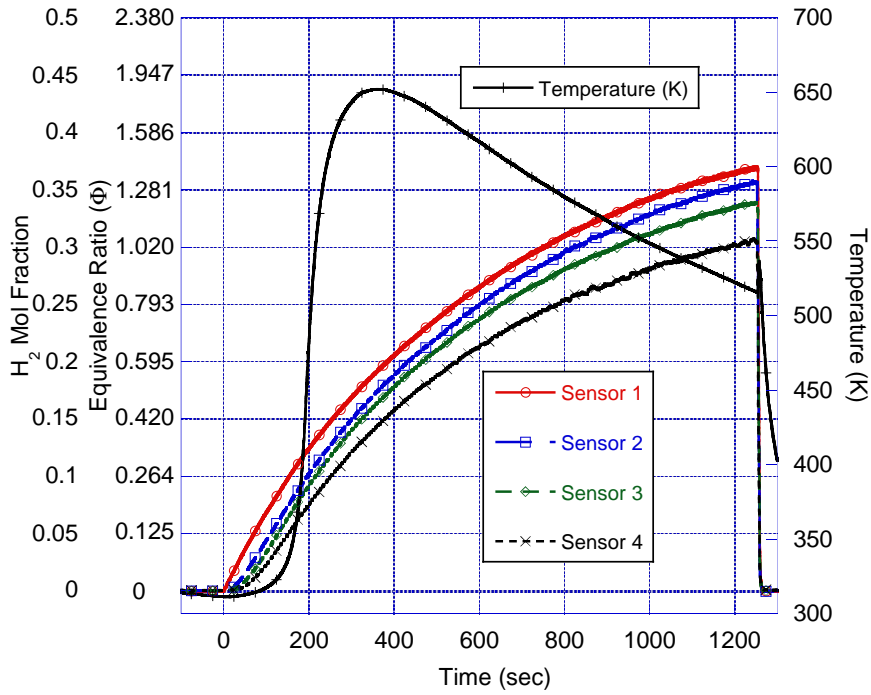


Figure 26: Characteristic temperature and hydrogen concentration response for a hydrogen flow rate of 0.0015 g/s. Catalyst is located 11.5 cm above the garage floor, 9 cm offset from the inlet.

To this point, the surface temperature at the onset of catalytic ignition (observed as a dramatic increase in surface temperature) has not been discussed. In Figs. 25 and 26, it can be seen that at time $t = 0$, when hydrogen is introduced into the chamber, that the surface temperature is slightly in excess of 300 K. However, in all cases tested with both inlet conditions, surface reactions are initiated directly from room temperature or slightly above (i.e. near 300 K). This behavior is in stark contrast to the results observed using the stagnation-point flow experiment to determine catalytic ignition temperatures, where room-temperature ignition was only observed for $\Phi < 0.2$. The reason for this differing of behavior may be explained by reference to Fig. 11. While at higher stretch rates the

ignition temperature does not seem to vary significantly with variation in flow conditions, as the stretch rate decreases towards zero, a significant drop in catalytic ignition temperature is observed. Extrapolating this trend to $k = 0 \text{ s}^{-1}$ would suggest that room temperature ignition could be observed for equivalence ratios normally requiring elevated surface temperature. In fact, this sort of behavior is observed in the simulated garage, where flow past the catalyst surface is minimal or negligible depending on its position relative to the inlet.

Despite this behavior, catalytic ignition in the current configuration is highly sensitive to initial conditions, specifically the surface condition of the catalyst and the surface temperature. As mentioned in Section 3.1.1.6, morphological changes in the platinum foil were observed over time in that experiment which resulted in a noticeable decrease in catalytic ignition temperatures. Similarly, on a day-to-day basis the surface condition may change slightly via processes such as contamination by trace gases in air or changes in surface oxidation. The result can be significant and unpredictable variations in observed ignition temperatures. In addition, even though surface reactivity may be observed, a specific case may “fizzle”, and the surface will return to room temperature instead of proceeding to an elevated steady state should an increase in surface temperature proceed too slowly relative to an increase in ambient hydrogen concentration. As a result, the only observation regarding catalytic ignition temperatures in the simulated garage is that ignition can occur at or near room temperature for a platinum surface across all equivalence ratios and pure hydrogen flow rates tested.

3.3.2 *Catalyst Surface Temperature Variations*

Before detailing the variations in surface temperature observed with varying flow conditions, it is important to discuss the dispersion of hydrogen within the garage for the varying flow conditions, as well as any impact that the catalyst may have on the hydrogen concentration. Figure 27 shows a series of hydrogen concentration measurements for equivalence ratios between $\Phi = 0.2$ and 0.8, with and without a catalyst located in the garage. Since all hydrogen concentration measurements converge to essentially a single value for the premixed inlet condition, only a single sensor history is used. At time $t = 0$, the premixed flow at the given equivalence ratio and 0.1 g/s mass flow rate is introduced into the garage. As is evident, the initial rise in hydrogen concentration increases significantly as equivalence ratio is increased. However, all equivalence ratios appear to approach steady-state concentration at approximately the same time. That the time to achieve steady-state is largely independent of equivalence ratio suggests that inlet mass flow rate and venting play a more significant role than inlet composition. With regards to steady-state composition within the garage, all cases without a catalyst approach the value at the inlet, with small downward deviations that can most likely be associated with preferential venting of hydrogen due to its high diffusion velocities. More importantly, very little deviation in steady-state hydrogen mole fraction, and negligible differences in form are observed between cases with and without a catalyst. In fact, at steady-state the deviation in mole fraction between the two situations is less than ~ 0.01 for all equivalence ratios tested. Importantly, this fact allows for surface temperature measurements to be discussed in light of general hydrogen concentration measurements

instead of the measurements associated with that particular test run. As a result, general trends can be discussed in later sections.

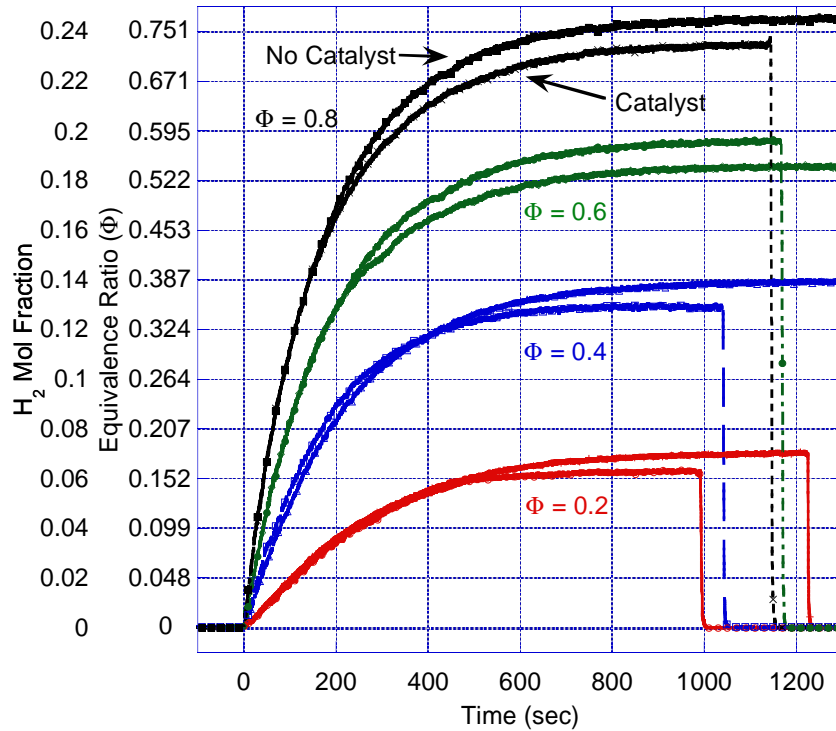


Figure 27: Comparison of hydrogen concentration measurements for cases with and without a catalyst for a premixed inlet flow condition at 0.1 g/s. Equivalence ratios between 0.2 and 0.8 are shown.

Similarly, Fig. 28 compares hydrogen concentration measurements with and without the presence of a catalyst for flow rates of 0.0005 and 0.002 g/s. As can be observed, the situation for a hydrogen-only inlet condition is the same as for the premixed condition. No discernable differences exist in the form of the concentration history, nor does the separation between sensor measurements appear to be affected. As before however, tests including a catalyst do result in minor reductions in hydrogen concentration throughout the garage.

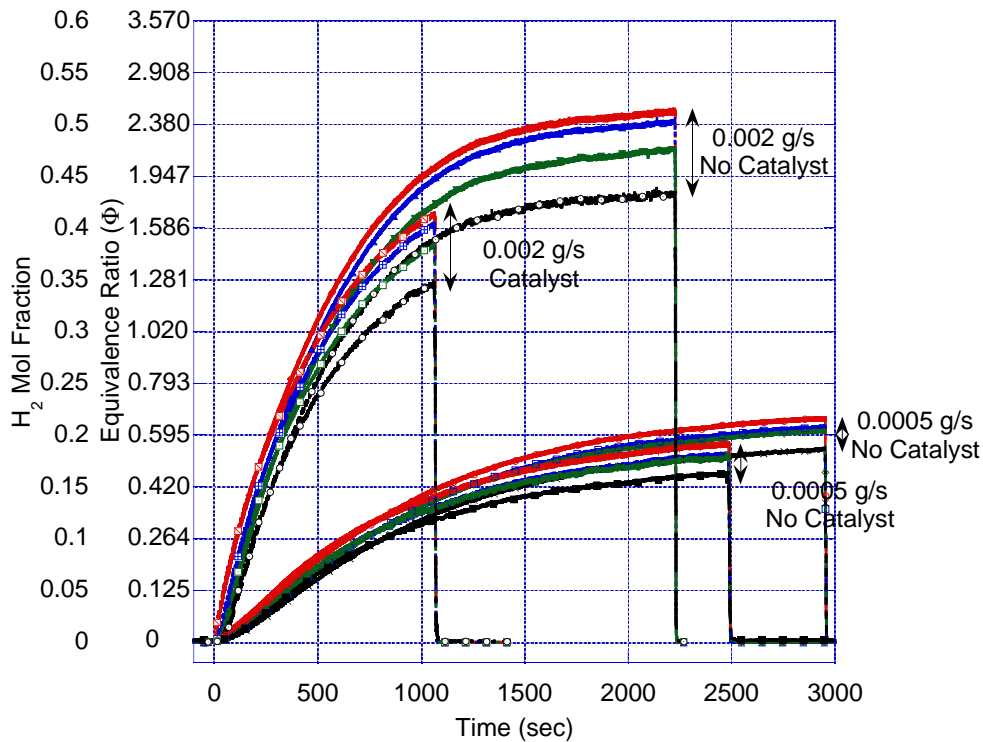


Figure 28: Comparison of hydrogen concentration measurements for cases with and without a catalyst for a hydrogen-only inlet flow condition. Flow rates of 0.002 and 0.0005 g/s are shown.

Figure 29 shows a series of temperature histories for a premixed inlet condition with an equivalence ratio between $\Phi = 0.2$ and 1.0. As with the premixed inlet condition in the previous section, the inlet total flow rate is 0.1 g/s, while the catalyst for these cases is located 6 cm above the garage floor and 9 cm offset from the inlet. For the lowest equivalence ratio $\Phi = 0.2$, after the mixture begins to flow into the garage at time $t = 0$ the surface temperature does not rise substantially until 300 seconds, where the temperature begins to quickly rise to a plateau near 700 K. In comparison, as the equivalence ratio is increased, this time delay decreases monotonically, reaching its lowest value for $\Phi = 1.0$. As will be shown in detail in the next section, as the equivalence ratio of the inlet flow increases, hydrogen concentration rises significantly

faster during the first few minutes following $t = 0$. This may help to explain the decrease in time delay with increasing equivalence ratio, as the fast rise in hydrogen concentration quickly removes any fuel-lean limitations on the catalytic surface reactions. The result is that the time delay is primarily a function of intrinsic thermal properties of the catalyst assembly rather than a combination of intrinsic and ambient conditions. It is also interesting to note the large gap in time delay occurring between $\Phi = 0.3$ and 0.4 , separating two groups consisting of $\Phi = 0.2$ and 0.3 , and $\Phi = 0.4$ to 1.0 . This time delay gap occurs at a quite similar equivalence ratio to the transition behavior discussed in Section 3.1.1.3, which may provide additional evidence suggesting the existence of two catalytic ignition regimes.

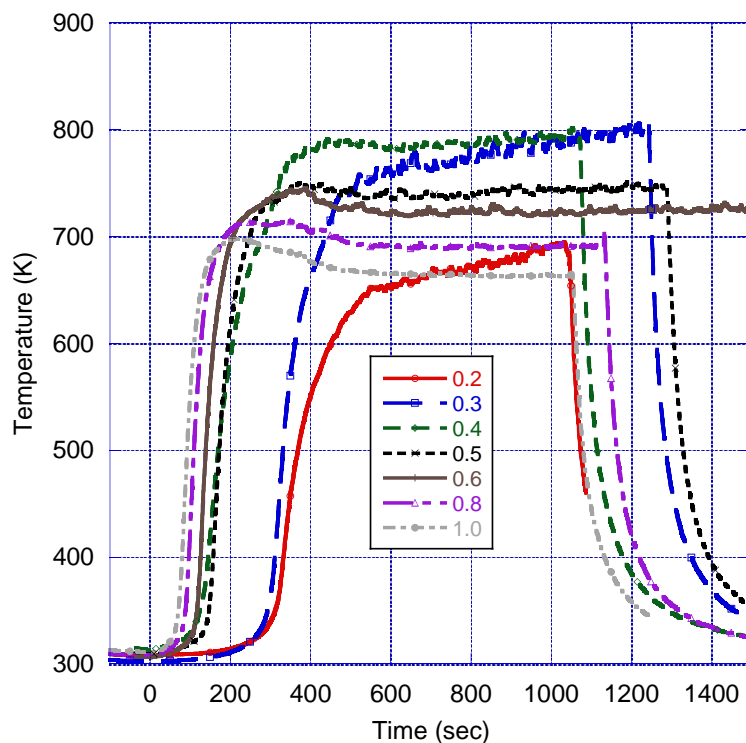


Figure 29: Characteristic temperature histories for various pre-mixed inlet equivalence ratios between $\Phi = 0.2$ and 1.0 at 0.1 g/s. The catalyst is located 6 cm above the garage floor and 9 cm offset from the inlet for these cases.

In addition to differences in time delay, varied equivalence ratio significantly impacts the post-ignition surface temperature achieved. For $\Phi = 0.2$, the surface temperature reaches to approximately 700 K (Fig. 29) and increases to 800 K as equivalence ratio increases to $\Phi = 0.3$ and 0.4. However, as equivalence ratio increases further to $\Phi = 0.5$ and beyond, surface temperature initially peaks following ignition and reaches a steady value that steadily decreases as hydrogen content of the flow increases. This behavior suggests that within the fuel-lean regime, an “ideal” equivalence ratio exists near $\Phi = 0.3$ to 0.4 that maximizes the surface temperature achieved. Since for the premixed inlet condition all elevations within the garage have essentially the same hydrogen concentration, this result should be largely independent of position within the garage, with the exception of the area immediately above the inlet.

To help determine the nature of any positional effects on achieved surface temperature, Fig. 30 shows the maximum achieved surface temperatures for four different positions within the garage. A single position is located 11.5 cm above the inlet, while the remaining three positions are located 9 cm horizontally offset from the inlet at heights of 11.5, 6, and 1 cm from the garage floor. When centered above the inlet, maximum surface temperatures increase from ~900 K at $\Phi = 0.2$ to almost 1100 K as equivalence ratio increases to $\Phi = 0.4$ and beyond. In contrast, when the catalyst is located in the offset position, regardless of height, temperature increases from ~700 K at $\Phi = 0.2$, increasing to a maximum near 800 K between $\Phi = 0.3$ –0.4 before falling as equivalence ratio increases further. That these trends are preserved for all heights provides further confirmation that only negligible differences in hydrogen concentration exist at varying heights within the garage for the premixed inlet condition. Additionally,

the variation in behavior between the offset and centered horizontal positions indicates that some amount of flow is forced against the catalyst surface in the centered position, which results in elevated surface temperatures observed relative to the offset position.

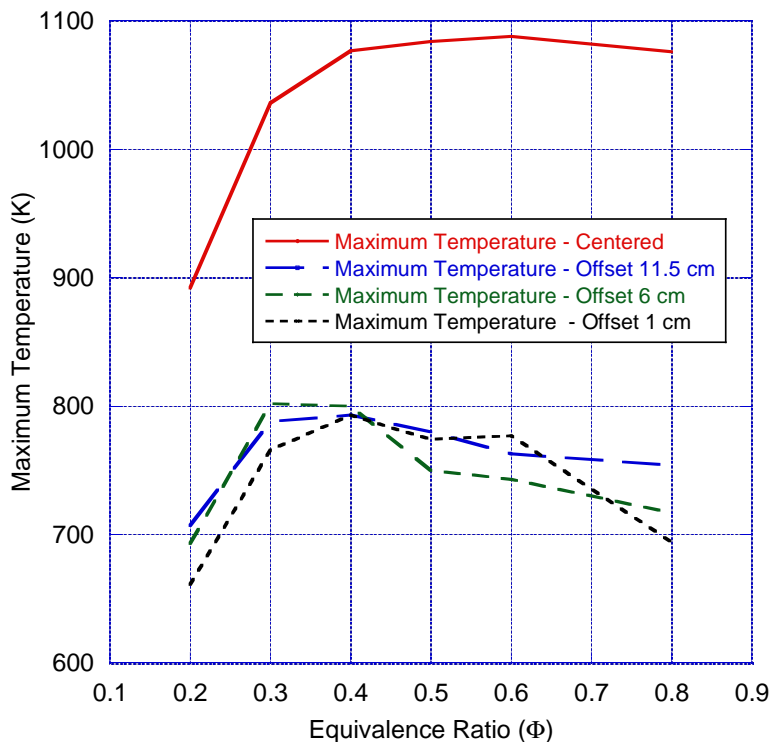


Figure 30: Maximum surface temperatures achieved for an inlet condition of 0.1 g/s and equivalence ratios between $\Phi = 0.2$ and 0.8. Centered refers to the catalyst located 11.5 cm above the garage floor, directly above the inlet. Offset refers to the catalyst being located 9 cm horizontally offset from the inlet, at the height listed in the figure.

A comparison similar to the previous discussion is shown in Fig. 31 for a hydrogen-only inlet condition at several mass flow rates between 0.0003 and 0.002 g/s. For 0.0003 g/s, the time required to observe thermal runaway on the catalyst surface is quite long relative to all the other cases shown. At least in part, this is likely due to the elongated time to reach a given hydrogen mole fraction (see Fig. 28). Though ignition begins with minimal surface reactions as soon as hydrogen reaches the catalyst surface, a significant amount of time is required for hydrogen to reach appreciable levels near the floor of the

garage. Therefore, it would be expected that as the hydrogen flow rate is increased, the induction time observed would decrease monotonically. In practice, this is the trend that is observed. An additional difference between the 0.0003 g/s case and all others tested can be observed in the long-term temperature profile; whereas most flow rates result in a temperature history exhibiting a peak after an initial thermal runaway followed by a reduction in surface temperature, no peak is observed for the 0.0003 g/s case. As flow rate is increased, the peaking behavior becomes increasingly dramatic, with monotonic reductions in peak temperature after 0.0005 g/s and increasingly steep temperature fall-off after the peak temperature is achieved. Since the steady-state hydrogen concentration as well as the initial rising rate increases with increased inlet flow rate, it can be concluded that an “ideal” concentration – much like what has been observed previously for premixed cases – exists, beyond which the peak temperature decreases.

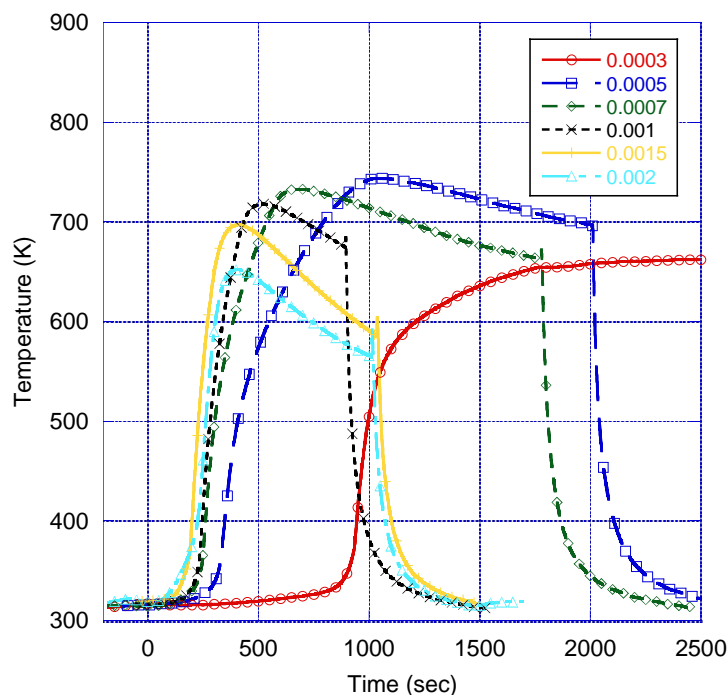


Figure 31: Characteristic temperature histories for various hydrogen inlet flow rates between 0.0003 and 0.002 g/s. The catalyst is located 1 cm above the garage floor and 9 cm offset from the inlet for these cases.

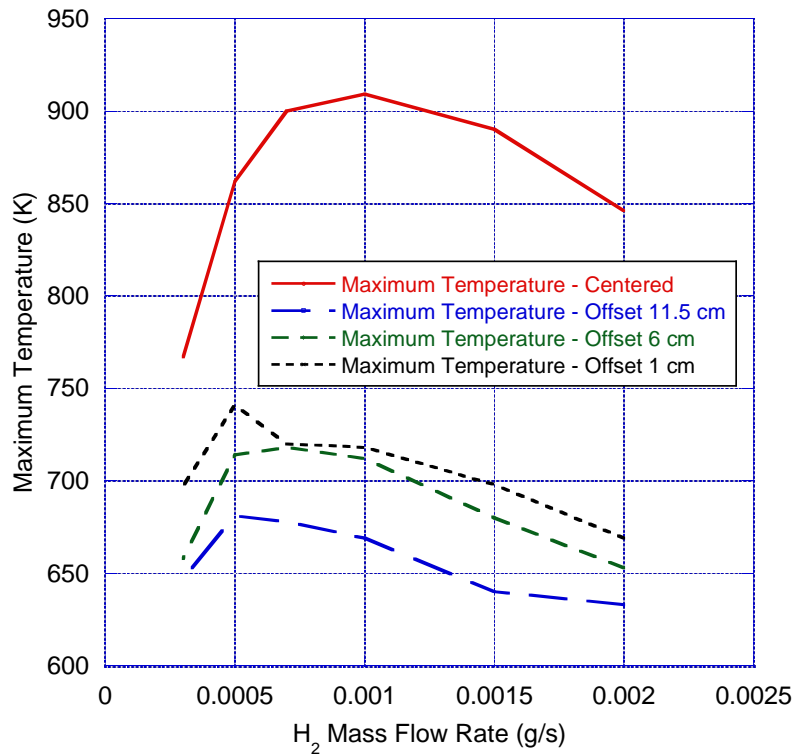


Figure 32: Maximum surface temperatures achieved for a hydrogen flow rates between 0.0003 and 0.002 g/s. Centered refers to the catalyst located 11.5 cm above the garage floor, directly above the inlet. Offset refers to the catalyst being located 9 cm horizontally offset from the inlet, at the height listed in the figure.

This behavior is confirmed by observing the peak catalyst surface temperatures reached for various flow rates at several locations within the garage (Fig. 32). In the centered position, as was seen for the premixed case, the peak temperature is significantly higher than is observed in the offset cases. Unlike the premixed inlet condition, however, as hydrogen flow rate is increased (compared to increased equivalence ratio at the same flow rate), the peak temperature is appreciably reduced, with the highest temperature achieved for a flow rate of 0.001 g/s. Also breaking with the premixed condition is the behavior observed in offset position. As height from the garage floor is decreased, a distinct monotonic increase in maximum temperature is observed, resulting in a ~50 K difference in peak surface temperature between the top and bottom of the garage. This

behavior demonstrates the surface temperature implications of the level of stratification within the garage for a hydrogen inlet condition. Importantly from a fire safety perspective, it indicates that despite the conventional wisdom that the hazard is located at an elevated height due to the rising hydrogen, at least for a catalytic ignition source a greater potential hazard may exist closer to the floor.

3.3.3 Effects of Varied Venting Conditions

To this point, a single venting condition has been used to demonstrate how hydrogen concentration interacts with a catalytic surface. The next important question for fire safety purposes is how various venting conditions may impact the hydrogen concentration within the garage. To this end, several venting conditions have been tested that aim to investigate the impact of venting location and total venting area. For all previously-discussed results, the venting condition consisted of two ¼ inch diameter holes located in the top and bottom of one corner of a wall. Added to this condition are the following venting scenarios. For the purposes of description, the terms “front” wall and “back” wall will be used to indicate opposing walls.

- 1) Two ¼ inch diameter holes – two holes located in the top and bottom of the front wall.
- 2) Two ¼ in diameter holes – one located at the top of the front wall, one located in the bottom of the back wall in the diagonally opposite corner.
- 3) Four ¼ in diameter holes – two holes located in the top and bottom of the front wall, two holes in the top and bottom of the back wall in the diagonally opposite corner.

- 4) Two ½ in diameter holes – two holes located in the top and bottom of the back wall.
- 5) Two ½ in diameter holes – one located at the top of the back wall, one located in the bottom of the front wall in the diagonally opposite corner.
- 6) Four ½ in diameter holes – two holes located in the top and bottom of the front wall, two holes in the top and bottom of the back wall in the diagonally opposite corner.
- 7) One ½ in diameter hole – located at the top of the back wall.

Two important trends should be investigated in this data; the effect of increased venting area provided, and the effect of varied vent locations utilizing the same area. For the purposes of fire safety, both effects may be critical to the safe design of structures where a realistic threat of a hydrogen leak exists.

The effect of increased area is somewhat intuitive; increasing area should result in an increased ability to vent hydrogen and thus a lower hydrogen concentration. In Fig. 33(a), results for flow rates of 0.002, 0.001, and 0.0005 g/s are shown for the case 1 venting condition, while Fig 33(b) shows results for a case 4 condition. As can be seen by comparing two identical flow rates, 0.002 g/s for example, increasing the venting area by a factor of four resulted in an approximately factor of two decrease in the hydrogen mole fraction accumulated within the garage at all heights. While not an exact rule, considering this behavior is preserved for all cases tested, this may represent a reasonable “rule-of-thumb”. However, also of interest is the steady-state value of the hydrogen mole fraction achieved for each hole size. Recalling the results of Fig. 32, the maximum catalyst surface temperature was achieved at all heights for a flow rate of 0.0005 g/s, indicating

that the rate of reactant consumption was closest to ideal for those particular conditions. If we then compare the ultimate value of hydrogen concentration for the 0.0005 g/s case in Fig 33(a) to the various flow rate results in Fig 33(b), we observe that the steady-state values for the two higher flow rates are quite similar. This indicates that while the total amount of hydrogen in the garage is reduced for larger vent sizes, depending on the flow rate expected from a hydrogen leak, this may not improve the overall safety with respect to a catalytic ignition source. Also of interest is that the level of stratification within the garage does not appear to be highly dependent upon the hole size, as the separation between the sensor measurements remains effectively the same despite the fourfold increase in venting area.

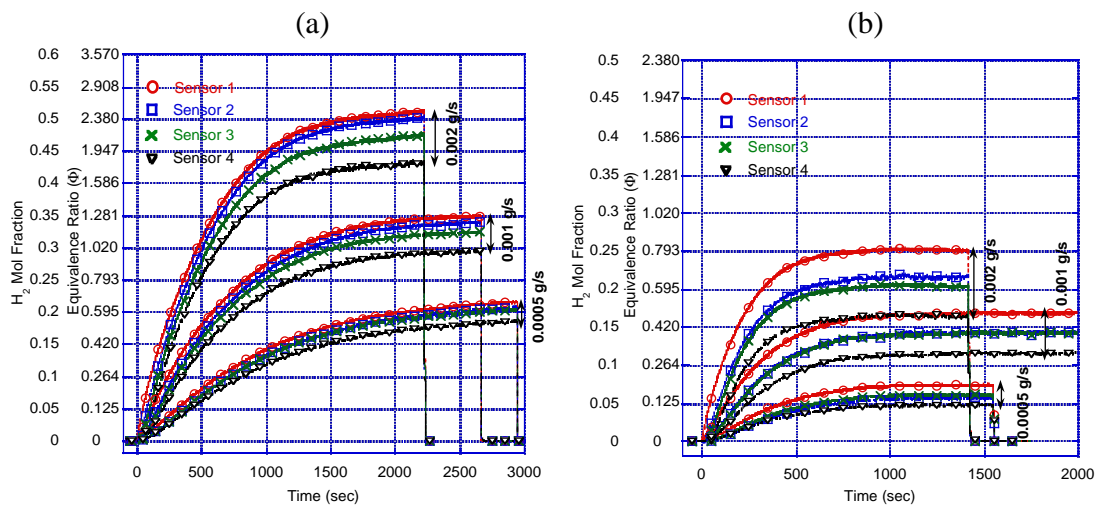


Figure 33: Comparison of hydrogen mole fraction measurements for 0.25 and 0.5 inch diameter holes arranged in the top and bottom of a single wall (case 1). Flow rates shown are 0.002, 0.001, and 0.0005 g/s. (a) 0.25 inch diameter holes. (b) 0.5 inch diameter holes.

The second trend of interest related to venting conditions is whether the arrangement of venting opportunities can impact the steady hydrogen concentration in the garage. Perhaps more so than the venting area, variations based upon the location of venting opportunities would be important in order to maximize their impact. Figure 34

demonstrates that differences in steady-state concentration can be affected by variations in the arrangement of venting opportunities. Referring to Fig. 34(a), where both 0.25 inch holes are located in the same wall, for a flow rate of 0.002 g/s the steady-state hydrogen mole fraction is just above 0.5, resulting in an equivalence ratio of $\Phi = 2.4$. However if the bottom hole is moved to the opposing corner at the same height, the result is shown in Fig. 34(b). Here the maximum mole fraction observed for a flow rate of 0.002 g/s reaches just above 0.55, an increase corresponding to an increase in equivalence ratio from $\Phi \sim 2.5$ to ~ 3.2 . This result is significant in that it suggests that if the primary goal of providing venting is to reduce the overall amount of hydrogen contained within the garage, careful consideration needs to be given not only to the size of vents, but where they are placed.

Considering a catalytic ignition source, it is noteworthy that in the preceding results, the surface temperature of the catalyst was maximized for a flow rate towards the low end of the range tested. Considering the results of this section, this dataset suggests that the fire safety hazard from a catalytic ignition source may be maximized for conditions where the hydrogen concentration remains within the lean regime for a long period of time. With regards to non-catalytic ignition sources, it is also interesting to note that many of the flow rate/venting combinations tested resulted in equivalence ratios that remained near $\Phi = 1$. This is significant in that these conditions more readily lend themselves to an explosion, a situation that would result in a significantly more destructive event. As a result, it may be important to consider the impact of hydrogen venting techniques in a specific application, as it is conceivable that some venting

conditions could actually contribute to a more dangerous situation than would otherwise be the case.

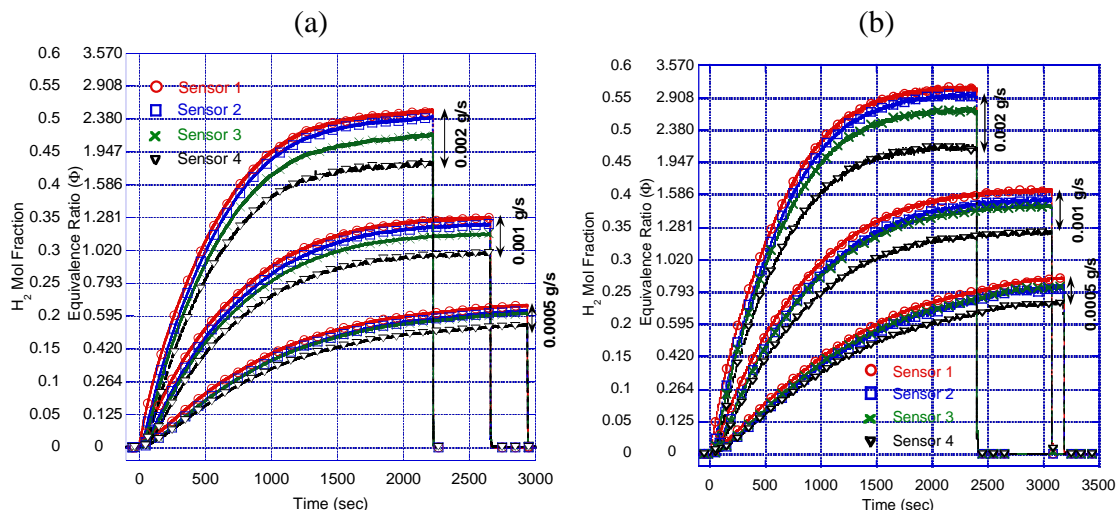


Figure 34: Comparison of hydrogen mole fraction measurements for two varying vent locations a) 0.25 inch diameter holes located at the top and bottom of a single wall (case 1). b) 0.25 inch diameter holes, one located in the top left corner of the front wall, one located in the diagonally opposed bottom corner. Flow rates shown are 0.002, 0.001, and 0.0005 g/s.

3.3.4 Additional Comments

In the preceding sections, all reactivity observed has been restricted to the surface, and for no situation within this dataset was a transition to gas-phase reactions observed. However, a transition to gas-phase reactions has been observed sporadically for some situations centered over the inlet. It is most probable that this behavior was not observed in the current dataset as a result of heat transfer considerations. For the purposes of attaching the catalyst surface to a polycarbonate arm protruding into the garage, an attachment bracket made of ceramic parts had to be included on the back side of the catalyst. This bracket added additional mass to the system, which would have impacted the heat transfer characteristics of the catalyst in the form of increased “thermal inertia” relative to some initial tests when a lightweight aluminum bracket was used. This

behavior illustrates the important point that while the temperature trends are expected to persist regardless of apparatus, the specific temperature values obtained will be sensitive to the mass and materials used as a result of heat transfer considerations.

4. Concluding Remarks

The experimental results presented in this report suggest several trends regarding hydrogen safety, both as it relates to a potential catalytic ignition source as well as ignition sources as a whole. From the stagnation-point flow and microtube experiments, datasets have been developed that may be applicable to situations where a flow is forced against a catalytic surface, while the scaled garage experiment provides significant data regarding situations where convective transport may be minimal. In addition, hydrogen dispersion data is presented which suggests several trends that may impact hydrogen safety regardless of the ignition source considered.

From the stagnation-point flow experiments, it is learned that for flows forced against a platinum surface, low equivalence ratios ($\Phi < 0.2$) exhibit ignition at room temperature, whereas at higher equivalence ratios (but still fuel-lean), elevated surface temperature ignition is observed approximately 60–70 K above room temperature. The separation between these two regimes appears to occur in the range of $\Phi = 0.3$ to 0.4, which is interesting considering that these conditions also appear to maximize the catalyst surface temperature achieved in the premixed scaled garage experiments. Overall, experiments seem to suggest that this equivalence ratio range separate two distinct regimes, considering both ignition and steady-state reactivity. However, it is unclear what

physical processes might underpin this observed behavior. Finally, it is observed that while the transition from surface to gas-phase reactions occurs somewhat unpredictably, the transition occurs near the top of reported gas-phase ignition temperature (900–1200 K), suggesting that the catalyst may not in any way serve to promote gas-phase reactions. In fact, considering computational work in the literature, it is possible that the presence of a catalyst may partially inhibit propagation into gas-phase by serving as a sink for radicals. While no evidence is presented here to support this hypothesis, it seems to reasonably explain the transition behavior observed.

Experiments using the microtube apparatus, while not greatly contributing to the understanding of ignition in this study, do help to elucidate the interaction between combustion behavior and heat transfer in the solid. While conditions in this experiment may have reasonably been expected to observe vigorous combustion, in cases of low flow rates or small tube diameter they did not. Most likely this is a result of the heat release rate from combustion being insufficient to overcome the heat loss through the solid. The important lesson for fire safety is that for a catalytic ignition source, the geometry and properties of the catalyst play as important a role as ambient conditions in any reactions that evolve.

Furthermore, the scaled garage system is used in an attempt to apply the knowledge gained in the previous experiments to a less well-characterized but more realistic scenario of hydrogen leaked into an enclosure containing a catalytic material. Most importantly, it is discovered that for all inlet conditions tested, catalytic reactions could proceed directly from room temperature or slightly above, suggesting that any platinum surface (or similar high-activity catalyst) has the potential to support surface reactions without the aid of

external heating. However, in most cases the reactions on the catalyst surface did not reach temperatures high enough to cause propagation from surface to gas-phase reactions. Once again, this appears to be related to the interplay of heat transfer and reaction rate. Similarly to the microtube experiments, heat transfer away from the catalyst surface appears to be sufficient in most situations to prevent a transition. However, some transitions to gas-phase are observed during testing using varied mounting methods. As a result, the possibility that a catalytic surface may serve as an ignition source for a gas-phase flame cannot be ruled out.

Finally, hydrogen dispersion experiments are carried out within the garage to observe how varied venting conditions might alter hydrogen concentrations. Based upon the results, it appears that for a catalytic ignition source, despite the commonly-held belief that due to hydrogen's tendency to rise the hazard zone it would be located at an elevated position, the opposite may be true. The catalyst appears to respond more strongly to fuel-lean conditions; conditions that, for a hydrogen-only leakage scenario, are replicated near the floor. In addition, hydrogen-only inlet conditions could easily result in equivalence ratios exceeding $\Phi = 1$. While common wisdom would dictate that reducing the total amount of hydrogen within an enclosure is preferable, some venting arrangements combined with flow rates result in steady-state hydrogen concentrations in the vicinity of $\Phi = 1$, a situation that maximizes the possibility of an explosion event. As a result, this experiment suggests that venting methods for an enclosure need to be paired with an estimated "most-likely" flow rate range in order to prevent the venting from contributing to, rather than detracting from, the danger posed by a hydrogen leak.

Appendix A

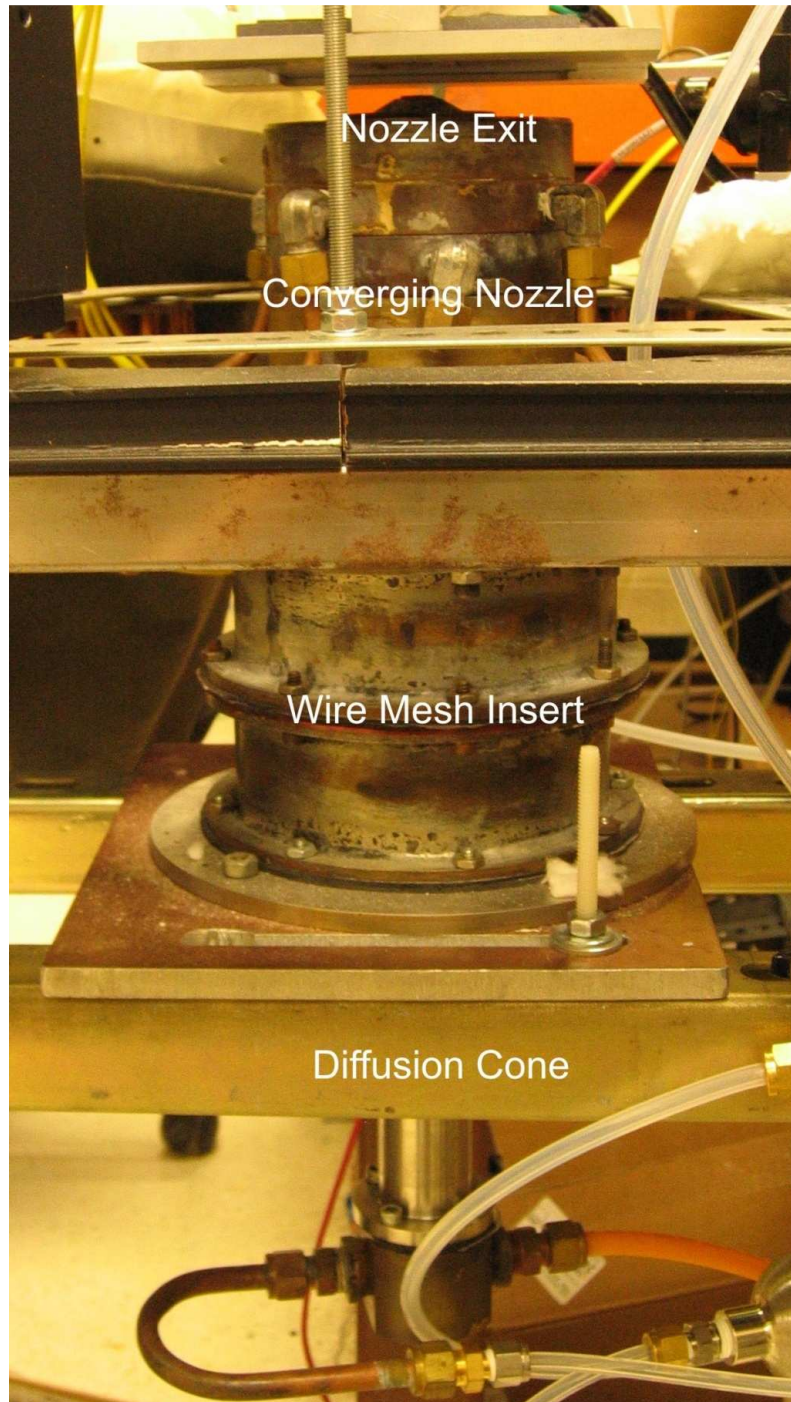


Figure A1: Photograph of the laminar flow burner assembly, with the location of major components shown. The stagnation assembly is located directly above the exit nozzle.

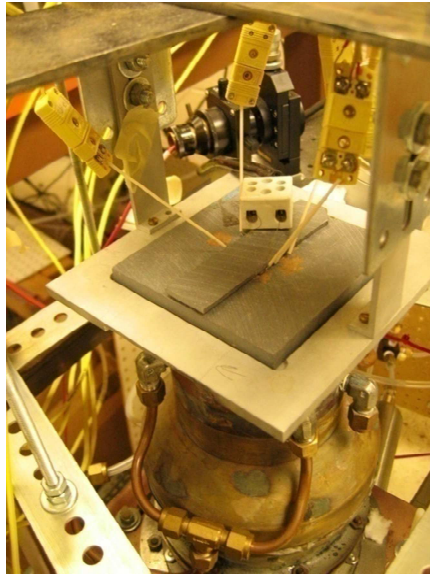


Figure A2: Photograph of stagnation assembly.

Appendix B

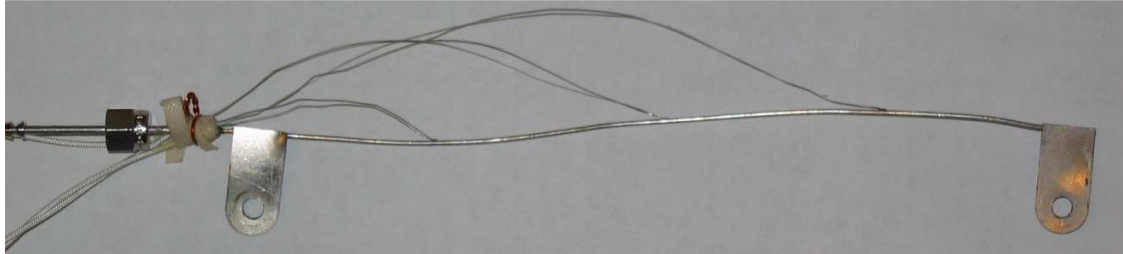


Figure B1: Photograph of 0.4 mm diameter platinum tube with thermocouples attached at 20%, 50%, and 80% of the 140 mm heated length.

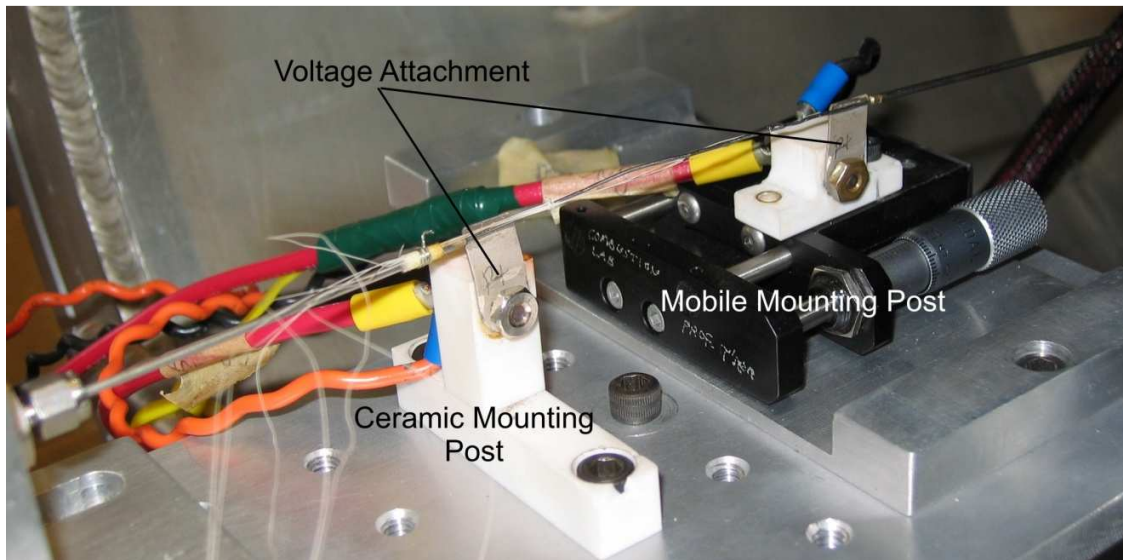


Figure B2: Mounting method for instrumented microtube. The nickel tabs are attached to the ceramic mounting posts, the second of which is placed on a translation stage to facilitate different size microtubes. The 0.4 mm microtube is shown.

List of Publications and Presentations

Journal Publication

K. B. Brady, C. J. Sung, and J. S. T'ien, "Ignition Propensity of Hydrogen/Air Mixtures Impinging on a Platinum Stagnation Surface," *International Journal of Hydrogen Energy* **35** (20), 11412-11423 (2010).

Manuscript in Preparation

K. B. Brady, C. J. Sung, and J. S. T'ien, "Dispersion and Catalytic Ignition of Hydrogen Leaks within Enclosed Spaces".

K. B. Brady, C. J. Sung, and J. S. T'ien, "An Investigation of Catalytic Activity of Metallic Surfaces in the Presence of Hydrogen Leaks".

Contributed Publications

K. B. Brady, K. Kumar, C. J. Sung, and J. S. T'ien, "Ignition Propensity of Premixed H₂/Air Mixtures in the Presence of a Platinum Surface," *Sixth Joint Meeting of the U.S. Sections of the Combustion Institute*, Ann Arbor, MI, 2009.

K. B. Brady, C. J. Sung, and J. S. T'ien, "Catalytic Ignition of Hydrogen Leaks within Enclosed Spaces," *Seventh Joint Meeting of the U.S. Sections of the Combustion Institute*, Atlanta, GA, 2011.

K. B. Brady, C. J. Sung, and J. S. T'ien, "Catalytic Ignition of Enclosed Hydrogen Leaks," *Fall Technical Meeting of the Eastern States Section of the Combustion Institute*, University of Connecticut, CT, 2011.

Presentations

C. J. Sung, "Ignition Propensity of Hydrogen in the Presence of Metal Surfaces," Annual Fire Conference, National Institute of Standards and Technology, Gaithersburg, MD, March 31, 2008.

K. B. Brady, "Ignition Propensity of Hydrogen in the Presence of Metal Surfaces," Ohio Space Grant Consortium, Cleveland, OH, April 20, 2008.

C. J. Sung, "Ignition Propensity of Hydrogen in the Presence of Metal Surfaces," Building and Fire Research Annual Fire Conference, Fire Measurement Method and Experimental Technique Workshop, National Institute of Standards and Technology, Gaithersburg, MD, April 29, 2009.

C. J. Sung, "An Evaluation of the Ignition Propensity of Hydrogen in the Presence of Metal Surfaces," Building and Fire Research Laboratory, National Institute of Standards and Technology, Gaithersburg, MD, May 18, 2010.

Thesis

K. B. Brady, "Ignition Propensity of Hydrogen/Air Mixtures in the Presence of Heated Platinum Surfaces," Mater Thesis, Department of Mechanical and Aerospace Engineering, Case Western Reserve University, January 2010.